

UNCLASSIFIED

AD 4 2 3 9 2 1

DEFENSE DOCUMENTATION CENTER

FOR

SCIENTIFIC AND TECHNICAL INFORMATION

CAMERON STATION, ALEXANDRIA, VIRGINIA



UNCLASSIFIED

NOTICE: When government or other drawings, specifications or other data are used for any purpose other than in connection with a definitely related government procurement operation, the U. S. Government thereby incurs no responsibility, nor any obligation whatsoever; and the fact that the Government may have formulated, furnished, or in any way supplied the said drawings, specifications, or other data is not to be regarded by implication or otherwise as in any manner licensing the holder or any other person or corporation, or conveying any rights or permission to manufacture, use or sell any patented invention that may in any way be related thereto.

CATLOGED BY DDC

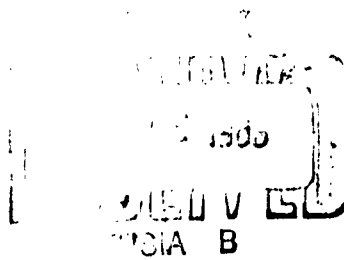
423927

AS 1.1.10.



MICROWAVE DEVICES LABORATORY
DEPARTMENT OF ELECTRICAL ENGINEERING

UNIVERSITY OF UTAH
SALT LAKE CITY, UTAH



Electronics Branch, Office of Naval Research
Department of the Navy, Washington 25, D. C.
Contract Nonr-1288(05)
Project NR 373-740
Millimeter Wave Devices

IMPEDANCE AND PROPAGATION CHARACTERISTICS
OF A FOUR COUPLED-LADDER BACKWARD-WAVE
OSCILLATOR WITH NONZERO PITCH

by

Lawrence S. Bowman and Richard W. Grow

Technical Report ONR-6
August 10, 1963

Reproduction in whole or in part
is permitted for any purpose of
the United States Government.

Microwave Devices Laboratory
Electrical Engineering Department
University of Utah
Salt Lake City, Utah

ABSTRACT

A general discussion of the theory of backward-wave oscillators is presented and the propagation and impedance characteristics are determined for a backward-wave oscillator having a circuit consisting of four coupled ladders placed across the narrow dimension of a waveguide. Propagation curves and impedance curves are presented for both the fundamental forward and the backward-wave components for several values of pitch and ladder plane spacing. A larger pitch or ladder plane spacing increases the frequency corresponding to a given phase constant.

The results indicate that the coupled-ladder backward-wave oscillator can be an effective source of microwave power.

TABLE OF CONTENTS

| | | |
|------|---|----|
| I. | INTRODUCTION | 1 |
| II. | THEORY OF BACKWARD-WAVE OSCILLATORS | 3 |
| | 2.1 Physical Basis of Operation | 3 |
| | 2.2 General Theory of Oscillation | 5 |
| III. | THEORY OF COUPLED LADDERS | 13 |
| | 3.1 Dispersion Characteristics | 13 |
| | 3.2 Impedance Characteristics | 33 |
| IV. | DISCUSSION OF RESULTS AND CONCLUSIONS | 54 |
| | REFERENCES | 55 |

LIST OF ILLUSTRATIONS

| FIGURE | PAGE |
|--|------|
| 1. Single Infinite Conducting Ladder Plane | 3 |
| 2. Backward-Wave Transmission Line and Beam | 6 |
| 3. Basic Interaction Cell Formed by Two Infinite Ladder Planes and Two Symmetrically-Placed Side Planes | 15 |
| 4. Slow-Wave Circuit Consisting of Four Coupled Ladder Across the Narrow Dimension of a Waveguide | 18 |
| 5. Propagation Constants for Four Coupled Ladder Planes in 2:1 Waveguide | 34 |
| 6. Propagation Constants for Four Coupled Ladder Planes in 2:1 Waveguide | 35 |
| 7. Forward-Wave Impedance at the Center of the Outer Ladder for Four Coupled Ladders in 2:1 Waveguide | 44 |
| 8. Forward-Wave Impedance at the Center of the Outer Ladder for Four Coupled Ladders in 2:1 Waveguide | 45 |
| 9. Backward-Wave Impedance at the Center of the Outer Ladder for Four Coupled Ladders in 2:1 Waveguide | 46 |
| 10. Backward-Wave Impedance at the Center of the Outer Ladder for Four Coupled Ladders in 2:1 Waveguide | 47 |
| 11. Variation of Interaction Impedance Across the Beam at the Center of the Ladder Planes for the Backward Wave | 50 |

I. INTRODUCTION

Oscillators have long been the subject of research and particular interest has been shown in extending their operation to higher frequencies. Backward-wave oscillators,¹ whose principle of operation will be described briefly in the following section, have been constructed at microwave frequencies and at millimeter wavelengths. Some of their advantages include wideband operation and ease of tuning using only one voltage. They may also become important sources of submillimeter waves.

Helices have been used as the slow-wave circuit in a number of backward-wave oscillators.² To increase the power output of traveling-wave tubes, Putz and Van Hoven³ suggested paralleling helices, which they did in 2-, 4-, and 9-helix arrays. Another type circuit that lends itself readily to parallel arrays is the ladder circuit. A successful oscillator using a ladder-type circuit was reported by Karp^{4,5} who obtained oscillations at 1.5 millimeters. Convert⁶ has successfully operated backward-wave oscillators using comb or vane-type circuits consisting essentially of half ladder planes in the submillimeter region. Paralleling of ladder planes has been considered by a number of authors^{7,8,9} and is the configuration of interest in this paper.

The fact that the axial electric field is enhanced and also extended in area by placing several ladder planes together so that the fields couple leads to an increase in the effective interaction impedance and hence to an increase in the power output.¹⁰ At millimeter wavelengths this property of coupled ladders becomes even more attractive because the field strength from a single

¹ Superscript numerals refer to the References which appear at the end of this of this report.

ladder dies off so rapidly on each side of the ladder plane. The purpose of this investigation is to explore the feasibility of constructing a coupled-ladder oscillator at millimeter and submillimeter wavelengths.

Section II describes the general theory of backward-wave oscillators and Section III contains the specialized theory of propagation and impedance characteristics of four coupled ladder planes in a waveguide. The discussion of results and conclusions appear in Section IV.

II. THEORY OF BACKWARD-WAVE OSCILLATORS

The following two sections describe the physical basis for the operation of backward-wave oscillators and give a brief theoretical derivation of the determinantal equations for oscillation. A number of parameters that are important in analyzing oscillator performance are defined.

2.1 Physical Basis of Operation

A periodic circuit such as the ladder plane shown in Fig. 1 can be used

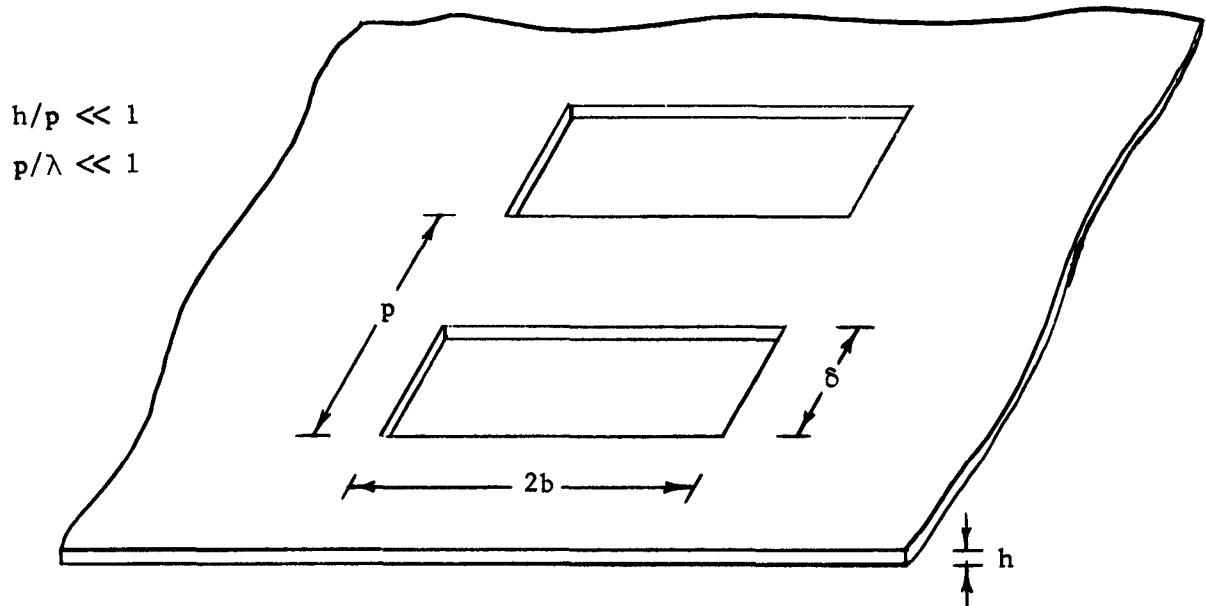


Fig. 1. Single infinite conducting ladder plane.

as a delay line or slow-wave circuit to support the propagation of an infinite number of electromagnetic waves moving in either direction with phase velocities less than the velocity of light. A backward wave is a wave which has its phase

and group velocities in opposite directions. If the velocity of an electron stream as determined by the beam voltage is approximately synchronized with the phase velocity of a backward wave, the wave moving in the reverse direction increases in energy so that a signal introduced at the collector end can be amplified. For sufficiently high current density in the electron beam and for a given length of circuit, the gain becomes infinite and oscillations will occur. A tube constructed to take advantage of this method of operation is called a backward-wave oscillator.

A picture of the operation of the oscillator can now be formulated. When the electrons in the beam encounter the strong r-f fields near the output of the tube at the gun end, they are speeded up or slowed down according to whether the axial electric field of the circuit is positive or negative. Thus, the electron beam acquires velocity and current modulation. The modulated beam traveling near the slow-wave circuit gives up kinetic energy to the circuit wave traveling at about the same velocity as the beam. The interaction between the circuit and the electron beam is strong only for frequencies having the phase velocity near the electron velocity. By limiting the current only the lowest mode of operation will be excited and a single output frequency will be obtained. Since backward-wave circuits are always dispersive with the phase velocity being a function of frequency the frequency of operation may be tuned by changing the beam voltage.

Since the strength of the fields diminishes rapidly away from the circuit, only those electrons immediately adjacent to the circuit are strongly affected by the circuit fields. Fuller utilization of the power in the electron beam

and hence higher efficiency and power output can be realized if the transverse area of high fields extends over more electrons. Parallel ladder planes placed close together so that the fields couple strongly offer a large area of high interaction impedance when flooded with electrons and hence offer the possibility of high power output from such an oscillator.

2.2 General Theory of Oscillation

The theory of operation of backward-wave oscillators has been discussed by many authors.^{11,12,13,14,15,16,17} Following Pierce, a brief small-signal steady-state analysis of backward-wave oscillators is developed by considering separately the effects on a transmission line of an adjacent electron beam (circuit equation) and the effects on the beam due to the fields of the transmission line (electronic equation). These two equations are combined to find the propagation constant of the combination. The oscillation condition in this section for a backward-wave oscillator is derived by allowing the backward-wave gain to be infinite. In later sections specific results for a coupled-ladder backward-wave oscillator are obtained.

The circuit equation is derived by considering an infinite backward-wave transmission line with shunt admittance per unit length Y and with series impedance per unit length Z shunted by an electron beam with total convection current i moving with velocity u_0 in the plus z -direction as shown in Fig. 2. The group velocity v_g is in a direction opposite to that of the phase velocity v_p for the backward waves. There will be a displacement current i per unit length flowing from the beam to the circuit to change the picture from that of the ordinary transmission line.

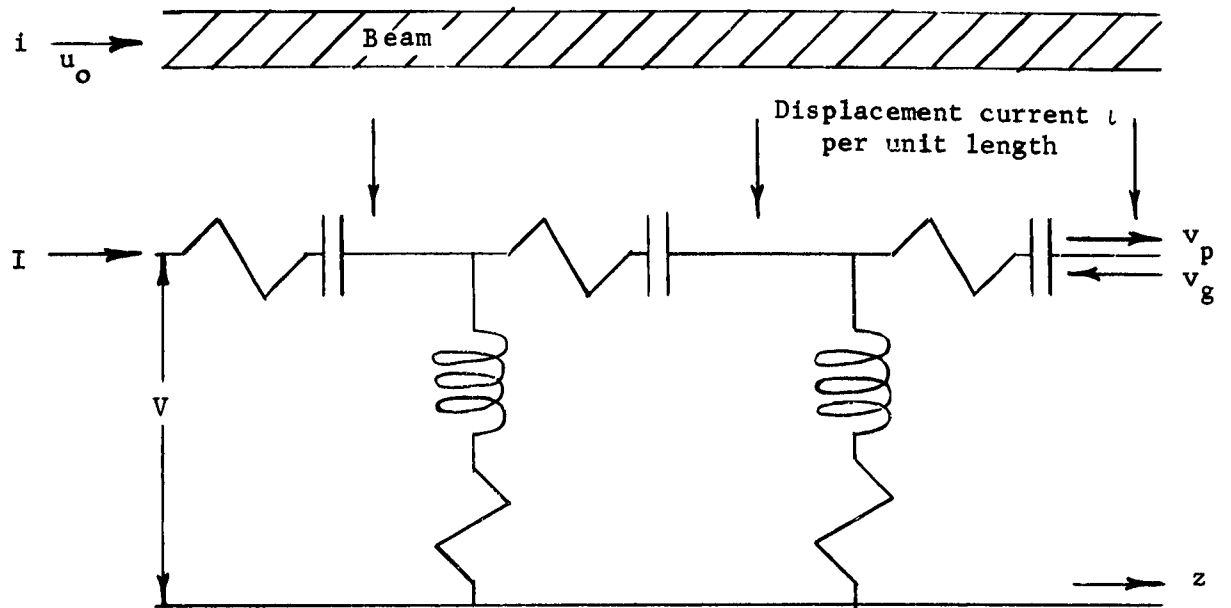


Fig. 2. Backward-wave transmission line and beam.

Because the group velocity is in the minus z -direction, energy flow is also in the minus z -direction and the differential equations for the transmission line become

$$\frac{\partial V}{\partial z} = ZI$$

$$\frac{\partial I}{\partial z} = YV + i \quad i = - \frac{\partial i}{\partial z}$$

where a term has been added to account for the displacement current from the beam. Combining the preceding equations we find that

$$\frac{\partial^2 V}{\partial z^2} - ZYV = -Z \frac{\partial i}{\partial z} \quad (2.1)$$

In the absence of an electron beam the right-hand side is zero and the

voltage solution is in terms of exponentials, depending upon the natural propagation constant of the line $\Gamma_o = \alpha_o + j\beta_o = (ZY)^{1/2}$. The impedance of the line can be defined as

$$K = (Z/Y)^{1/2} = Z/\Gamma_o$$

Propagation of the principal mode with the beam present will be assumed to vary as $\exp(j\omega - \Gamma z)$ where $\Gamma = \alpha + j\beta$ is the propagation constant of the coupled system. Let E represent the z-component of electric field. Then since

$$E = -\nabla \cdot \hat{z} = -\frac{\partial V}{\partial z} = IV$$

differentiation of Eq. 2.1 leads to the circuit equation

$$E = \frac{\Gamma_o \Gamma^2 K}{\Gamma^2 - \Gamma_o^2} i \quad (2.2)$$

By assuming that r-f effects are small compared with d-c effects, we may obtain the small-signal electronic equation by combining Maxwell's equations, the continuity equation for charge, and the Lorentz force equation as applied to an electron stream acted upon by an axial electric field E. This equation is

$$i = \frac{j\beta_e I_o / 2V_o}{(\Gamma - j\beta_e)^2 + \beta_q^2} E \quad (2.3)$$

where I_o is the d-c beam current and V_o is the beam voltage. The beam velocity u_o is related to the beam voltage through the equation

$$\frac{u_o}{c} = \frac{(2\eta V_o)^{1/2}}{c} = \frac{(V_o)^{1/2}}{506} \quad (2.4)$$

where η is the charge-to-mass ratio of the electron and c is the velocity of light. The term β_q^2 takes into account localized space-charge fields and may be shown to be expressible by

$$\beta_q^2 = \frac{\omega_q^2}{u_o^2} = \frac{R^2 \omega_p^2}{u_o^2} \approx \frac{I_o K \beta_e^2 Q}{V_o} \quad (2.5a)$$

where $\omega_p = (\eta J_o / \epsilon_o u_o)^{1/2} = 1.83 \times 10^8 J_o^{1/2} / V_o^{1/4}$ is called the plasma frequency and R is a reduction factor which is less than one and takes into account the finite beam size. J_o is the direct current density in the beam, $\beta_e = \omega / u_o$, and Q is called the space-charge parameter of Pierce. Since Pierce's gain parameter

$$C = \left(\frac{I_o K}{4V_o} \right)^{1/3} \quad (2.5b)$$

in most practical tubes is much less than one, Eq. 2.5a may be written

$$\omega_q \approx \omega (4QC^3)^{1/2} \quad (2.6)$$

The equation for the propagation constant Γ can now be obtained by combining Eqs. 2.2 and 2.3

$$1 = \frac{j2\beta_e c^3 \Gamma_o \Gamma^2}{(\Gamma^2 - \Gamma_o^2) \left[(\Gamma - j\beta_e)^2 + \beta_q^2 \right]} \quad (2.7)$$

The parameter d , which is related to the cold circuit loss, and the synchronism parameter b will now be introduced and Eq. 2.7 will be reduced to a simpler expression. As the circuit waves should be approximately synchronized with the beam waves, let

$$\Gamma_o = j\beta_e (1 + bc) - \beta_e Cd \quad (2.8)$$

and

$$\Gamma = j\beta_e - \beta_e C\delta \quad (2.9)$$

where the unknown quantity is δ and $C \ll 1$. Equation 2.7 now becomes

$$\delta^2 = \frac{1}{(b + jd) - j\delta} - 4QC \quad (2.10)$$

Letting the three solutions of Eq. 2.10 be designated by $\delta_1, \delta_2, \delta_3$, we find three propagation constants

$$\Gamma_v = j\beta_e - \beta_e C\delta_v, \quad v = 1, 2, 3$$

and three propagating waves

$$E(z) = \sum_{v=1}^3 E_v e^{-\Gamma_v z} \quad (2.11)$$

where the amplitude constants E_v may be found after boundary conditions are imposed.

The boundary conditions are that at the output end of the tube (at $z = 0$) the velocity and current modulation are zero. These two conditions together with Eq. 2.11 give three equations in the unknowns E_1, E_2, E_3 .

$$\sum_{v=1}^3 E_v = E(0) \quad (2.12a)$$

$$\sum_{v=1}^3 \frac{E_v}{\delta_v^2 + 4QC} = 0 \quad (2.12b)$$

$$\sum_{v=1}^3 \frac{\delta_v E_v}{\delta_v^2 + 4QC} = 0 \quad (2.12c)$$

The solutions of Eqs. 2.12 can easily be found in terms of $E(0)$ provided $b, d,$ and QC are known. The total uniform distributed loss ℓ in db may be related to the loss parameter d in a tube of length L (yet unspecified) by the equation

$$\ell = 20 \log_{10} \exp \beta_e C d L = 54.6 d C N \quad (2.13)$$

where $N = \beta L / 2\pi$ is the number of wavelengths in the length L . Since QC may be found in terms of known tube parameters by Eq. 2.5, only two

parameters in Eq. 2.11 remain unknown, b and CN , provided something can be done with $E(0)$.

If the tube is to oscillate, the gain must become infinite in length L

$$G = \left| \frac{E(0)}{E(L)} \right| \rightarrow \infty$$

and since $E(0)$ is finite, $E(L)$ must go to zero. Simultaneous solution of Eq. 2.10, together with the oscillation condition

$$\begin{aligned} E(L) = 0 &= \sum_{v=1}^3 E_v e^{-\Gamma_v L} \\ &= \frac{\delta_1^2 + 4QC}{(\delta_1 - \delta_2)(\delta_1 - \delta_3)} e^{\beta_e CL\delta_1} \\ &\quad + \frac{\delta_2^2 + 4QC}{(\delta_2 - \delta_3)(\delta_2 - \delta_1)} e^{\beta_e CL\delta_2} \\ &\quad + \frac{\delta_3^2 + 4QC}{(\delta_3 - \delta_1)(\delta_3 - \delta_2)} e^{\beta_e CL\delta_3} \end{aligned} \quad (2.14)$$

will thus determine CN and b for start oscillation with the given values of loss and space charge. Generally a length is decided upon which will be long enough to produce oscillations for the available beam voltage, and values of current required for start oscillation are then found from

the relationship

$$(CN)_{\text{start}} = \left(\frac{I_{\text{start}} K}{4 V_0} \right)^{1/3} N \quad (2.15)$$

From Eq. 2.8 the phase constant of the circuit wave is $\beta_e (1 + bC) = \omega/v$ so that the phase velocity $v = u_0 (1 + bC)$, and therefore the determined value of b makes it possible to find the frequency of oscillation from the dispersion characteristics of the circuit.

Consideration of the preceding results will indicate that there possibly is more than a single set of conditions for oscillation, and this turns out to be true as found by Walker.¹⁴ The higher order modes of oscillation can be avoided if the operating current is held to eight to ten times I_{start} .

In Section II, backward-wave oscillation has been considered first from a physical basis and second from a more quantitative viewpoint. The requirements for oscillation have been found for a backward-wave oscillator. The next step will be to determine the parameters of the coupled ladder circuit. In Section III, the dispersion and impedance characteristics of a coupled-ladder circuit will be obtained.

III. THEORY OF COUPLED LADDERS

In the following two sections the theoretical dispersion and impedance characteristics of four coupled ladder planes placed across the narrow dimension of a waveguide are derived. Curves are presented which show graphically the changes in dispersion and impedance due to variations in pitch and ladder plane spacing.

3.1 Dispersion Characteristics

The dispersion diagram indicates graphically the dependence of phase velocity on frequency and is commonly shown as an ω - β diagram with the frequency parameter as ordinate and phase constant as abscissa. In this work, $k = \omega/c_0$ will be plotted versus β , each normalized to the cutoff wave number $k_c = \omega_c/c = 2\pi/\lambda_c$. Normalizing the phase velocity v to the velocity of light, we obtain

$$\frac{v}{c} = \frac{k}{\beta} = \frac{k/k_c}{\beta/k_c} = \tan \psi \quad (3.1)$$

where ψ is the angle which a straight line through the origin and point of interest on the dispersion curve makes with the β/k_c axis. Use will be made of Eq. 3.1 in a later section when the beam voltage will be found as a function of frequency.

Consider the problem of a wave propagating axially down a lossless circuit which is periodic in the z -direction. Assume sinusoidal excitation with the phase reference propagating with a phase velocity v . The electric

field vector with the phase dependence separated out may be written in the form

$$\vec{E}(x, y, z, t) = \text{Re} \left[\vec{E}(x, y, z) e^{j(\omega t - \beta_0 z)} \right] \quad (3.2)$$

with $\beta_0 = \omega/v$. Since Eq. 3.2 shows the phase dependence separated out, the vector $\vec{E}(x, y, z)$ is a function of the geometry of the slow-wave circuit. The operator Re will not be written until it need be expressed explicitly later. A similar development holds for the magnetic field vector \vec{H} , with $\vec{H}(x, y, z)$ representing the geometrical function.

Appropriate forms for \vec{E} and \vec{H} will be needed which will satisfy Maxwell's equations and the boundary conditions in the lossless ladder cell consisting of two infinite conducting ladder planes of the type shown in Fig. 1 intercepting two symmetrically placed conducting side planes as shown in Fig. 3. The side planes have been placed a distance c from the center of the ladder slots. Effects of circuit loss will be introduced later.

Let \vec{E} be expanded into a longitudinal Fourier series¹⁸ with period p so that Eq. 3.2 becomes

$$\vec{E}(x, y, z, t) = \sum_{n=-\infty}^{\infty} \vec{E}_n(x, y, z, t) = \sum_{n=-\infty}^{\infty} \vec{E}_n(x, y) e^{-j(2\pi n z/p)} e^{j(\omega t - \beta_0 z)} \quad (3.3)$$

where $\vec{E}_n(x, y)$ is the function describing the variation of the n th axial space harmonic of $\vec{E}(x, y, z)$ with the transverse coordinates. It is

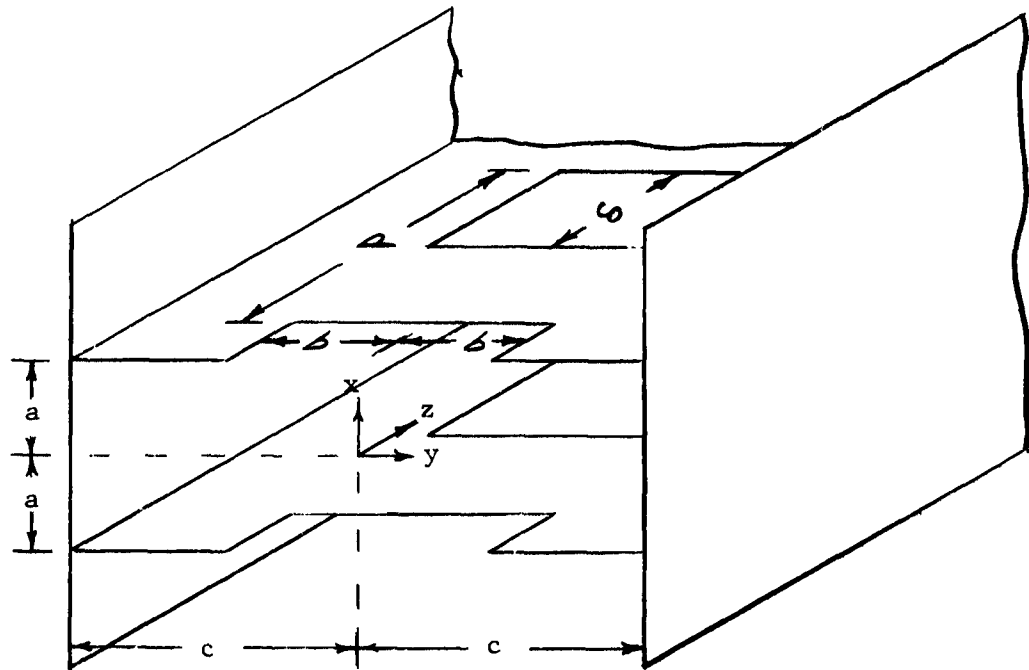


Fig. 3. Basic interaction cell formed by two infinite ladder planes and two symmetrically-placed side planes.

convenient here to define the phase constant of the n th space harmonic as

$$\beta_n = \beta_0 + \frac{2\pi n}{p} \quad (3.4)$$

with associated phase velocity $v_n = \omega/\beta_n$.

Since the ladder plane can be considered periodic in y (see Fig. 3) \vec{E} can also be expanded into a series of transverse space harmonics. The axial component of electric field with even excitation about the $y = 0$ plane becomes

$$\mathcal{E}_z(x, y, z, t) = \sum_{n=-\infty}^{\infty} \sum_{m=0}^{\infty} \mathcal{E}_{znm}(x, y, z, t) = \sum_{n=-\infty}^{\infty} \sum_{m=0}^{\infty} E_{znm}(x) \cos \zeta_m y e^{j(\omega t - \beta_n z)} \quad (3.5)$$

The axial component of the magnetic field vector is

$$\mathcal{H}_z(x, y, z, t) = \sum_{n=-\infty}^{\infty} \sum_{m=0}^{\infty} \mathcal{H}_{znm}(x, y, z, t) = \sum_{n=-\infty}^{\infty} \sum_{m=0}^{\infty} H_{znm}(x) \sin \zeta_m y e^{j(\omega t - \beta_n z)} \quad (3.6)$$

The factors $E_{znm}(x)$ and $H_{znm}(x)$ show the x-dependence of the n,m component of the axial electric and magnetic fields respectively.

Maxwell's curl equations and the orthogonality properties of the trigonometric functions give for the transverse fields¹⁹

$$\vec{\mathcal{H}}_{tnm} = \frac{1}{k^2 - \beta_n^2} \left[j\omega\epsilon \nabla_t \times \vec{\mathcal{E}}_{znm} - j\beta_n \nabla_t \mathcal{H}_{znm} \right] \quad (3.7a)$$

$$\vec{\mathcal{E}}_{tnm} = \frac{1}{k^2 - \beta_n^2} \left[-j\omega\mu \nabla_t \times \vec{\mathcal{H}}_{znm} - j\beta_n \nabla_t \mathcal{E}_{znm} \right] \quad (3.7b)$$

where

$$\nabla_t = \hat{x} \frac{\partial}{\partial x} + \hat{y} \frac{\partial}{\partial y} \quad (3.8)$$

The notation \hat{x} and \hat{y} indicates unit vectors in the x and y directions.

In the light of Eq. 3.7 all field quantities can be found as soon as

$E_{znm}(x)$ and $H_{znm}(x)$ are known. The boundary conditions will now be applied to determine ζ_m and β_n .

Consider now the ladder structure shown in Fig. 4. Let the ladder thickness be neglected (let $h \rightarrow 0$ in Fig. 1) and assume infinitely thin, perfectly conducting planes at $x = a$, $a + 2g$, and $a + 2g + d$. With three regions defined as in Fig. 4, $E_{znm}(x)$ and $H_{znm}(x)$ can be written in one-half the ladder structure and symmetry properties can be used for the other half. The field functions must satisfy the boundary conditions^{20,21}

$$\hat{u} \times (\vec{E}_{nm1} - \vec{E}_{nm2}) = 0 \quad (3.9a)$$

$$\hat{u} \cdot (\vec{H}_{nm1} - \vec{H}_{nm2}) = 0 \quad (3.9b)$$

$$\hat{u} \times (\vec{H}_1 - \vec{H}_2) = \vec{J}_s \quad (3.9c)$$

$$\hat{u} \cdot (\vec{E}_1 - \vec{E}_2) = \rho_s / \epsilon_0 \quad (3.9d)$$

where ρ_s is the surface charge density, \vec{J}_s is the surface current density and \hat{u} is a normal unit vector. In addition they must satisfy the wave equation everywhere

$$\nabla^2 \begin{Bmatrix} \vec{E}_{nm} \\ \vec{H}_{nm} \end{Bmatrix} = -k^2 \begin{Bmatrix} \vec{E}_{nm} \\ \vec{H}_{nm} \end{Bmatrix} \quad (3.10)$$

The boundary condition that at the conducting walls at $y = \pm c$ the tangential electric field must go to zero gives, using Eq. 3.5, that

$$\zeta_m = (2m + 1)\pi/2c.$$

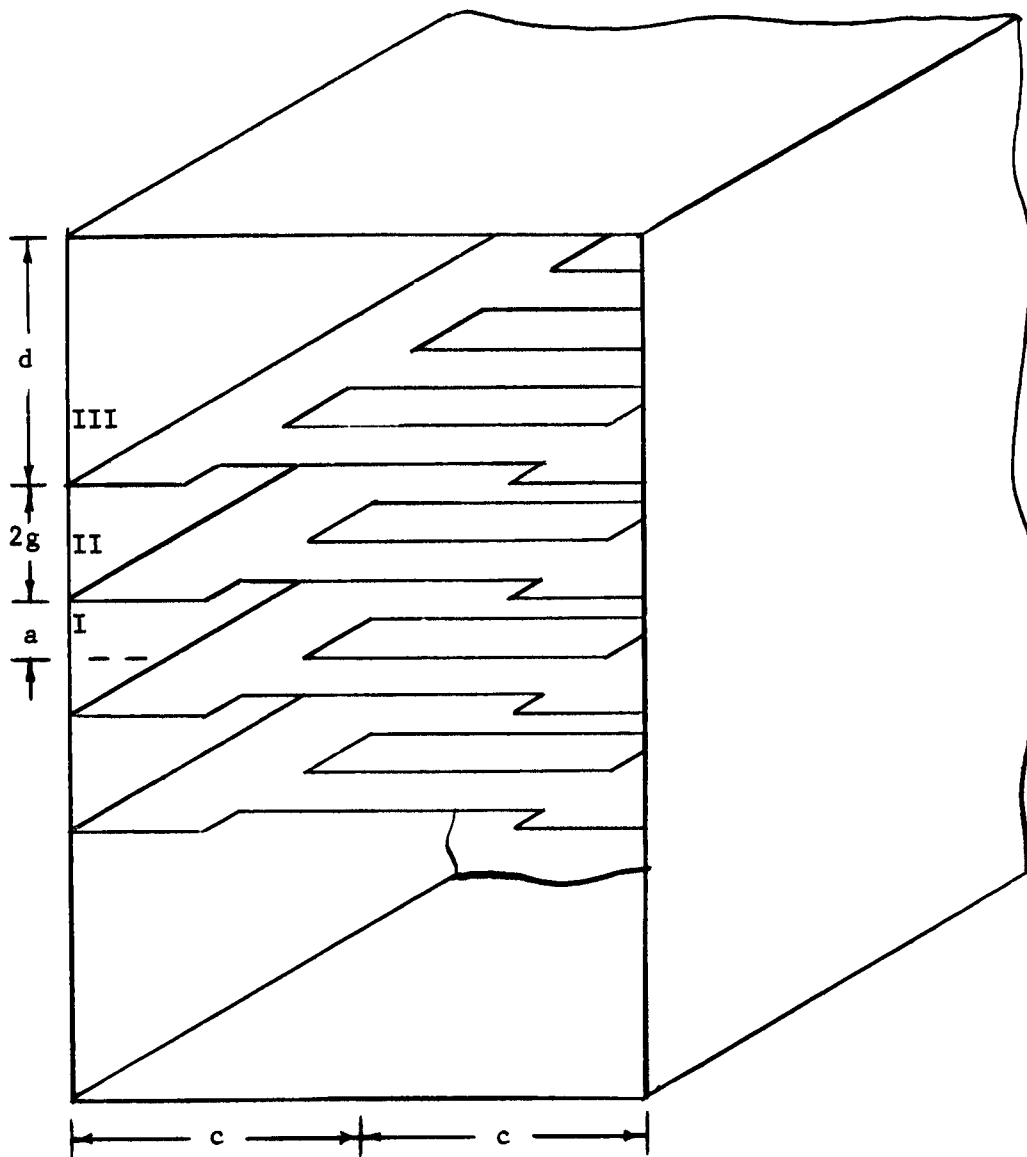


Fig. 4. Slow-wave circuit consisting of four coupled ladders across the narrow dimension of a waveguide.

With a Roman numeral superscript to designate the region the appropriate axial field functions for the longitudinal mode can be written with constants as indicated which will be found by application of the boundary conditions.

Region I:

$$E_{znm}^I(x) = A_{nm} \frac{\cosh \gamma_{nm} x}{\cosh \gamma_{nm} a} \quad (3.11a)$$

$$H_{znm}^I(x) = B_{nm} \frac{\sinh \gamma_{nm} x}{\cosh \gamma_{nm} a} \quad (3.11b)$$

Region II:

$$E_{znm}^{II}(x) = C_{nm} \frac{\cosh \gamma_{nm} [x - (a + g)]}{\cosh \gamma_{nm} g} + C'_{nm} \frac{\sinh \gamma_{nm} [x - (a + g)]}{\sinh \gamma_{nm} g} \quad (3.11c)$$

$$H_{znm}^{II}(x) = D_{nm} \frac{\sinh \gamma_{nm} [x - (a + g)]}{\cosh \gamma_{nm} g} + D'_{nm} \frac{\cosh \gamma_{nm} [x - (a + g)]}{\sinh \gamma_{nm} g} \quad (3.11d)$$

Region III:

$$E_{znm}^{III}(x) = F_{nm} \frac{\sinh \gamma_{nm} [x - (a + 2g + d)]}{\sinh \gamma_{nm} d} \quad (3.11e)$$

$$H_{znm}^{III}(x) = G_{nm} \frac{\cosh \gamma_{nm} [x - (a + 2g + d)]}{\sinh \gamma_{nm} d} \quad (3.11f)$$

where

$$\gamma_{nm}^2 = \beta_n^2 + \zeta_m^2 - k^2 \quad (3.12)$$

The electric field excitation will be assumed at the outside ladder plane ($x = a + 2g$) and will be considered to have a zero y-component since the presence of the conducting ladder plane would tend to short out the \mathcal{E}_y fields. The \mathcal{E}_y fields are thus everywhere zero and from Eq. 3.7 there follows

$$\frac{\partial \mathcal{E}_{znm}}{\partial y} = \frac{\omega \mu}{\beta_n} \frac{\partial \mathcal{H}_{znm}}{\partial x} \quad (3.13)$$

With the definition

$$\theta_{nm} = - \frac{\beta_n \zeta_m}{\omega \mu \gamma_{nm}} \quad (3.14)$$

it follows that

$$B_{nm} = \theta_{nm} A_{nm} \quad (3.15a)$$

$$D_{nm} = \theta_{nm} C_{nm} \quad (3.15b)$$

$$D'_{nm} = \theta_{nm} C'_{nm} \quad (3.15c)$$

$$G_{nm} = \theta_{nm} F_{nm} \quad (3.15d)$$

Also,

$$\frac{\partial H_{znm}}{\partial y} = \frac{\theta_{nm} \zeta_m}{\gamma_{nm}} \frac{\partial \mathcal{E}_{znm}}{\partial x} \quad (3.16)$$

and Eq. 3.7 now yields

$$H_{ynm} = \frac{\zeta_m^2 - k^2}{j\omega\mu \gamma_{nm}^2} \frac{\partial \mathcal{E}_{znm}}{\partial x} \quad (3.17)$$

With Eq. 3.9a the \mathcal{E}_z fields can be matched across each ladder plane to give

$$A_{nm} = C_{nm} - C'_{nm}$$

$$-F_{nm} = C_{nm} + C'_{nm}$$

which leads to

$$C_{nm} = \frac{1}{2} (A_{nm} - F_{nm}) \quad (3.18a)$$

$$C'_{nm} = -\frac{1}{2} (A_{nm} + F_{nm}) \quad (3.18b)$$

Equation 3.9c can now be used to assure continuity of the magnetic fields across the ladder planes. Because of the slots cut in the ladder

planes, there can be no axial current and thus

$$N_y^I(a, y, z, t) = N_y^{II}(a, y, z, t) \quad (3.19a)$$

$$N_y^{II}(a + 2g, y, z, t) = N_y^{III}(a + 2g, y, z, t) \quad (3.19b)$$

With Eq. 3.17 the H_{ynm} functions in the three regions are found to be

$$H_{ynm}^I(x) = \frac{\zeta_m^2 - k^2}{j\omega\mu\gamma_{nm}} A_{nm} \frac{\sinh \gamma_{nm} x}{\cosh \gamma_{nm} a} \quad (3.20a)$$

$$H_{ynm}^{II}(x) = \frac{\zeta_m^2 - k^2}{j\omega\mu\gamma_{nm}} \left[\frac{(A_{nm} - F_{nm}) \sinh \gamma_{nm} [x - (a + g)]}{2 \cosh \gamma_{nm} g} - \frac{(A_{nm} + F_{nm}) \cosh \gamma_{nm} [x - (a + g)]}{2 \sinh \gamma_{nm} g} \right] \quad (3.20b)$$

$$H_{ynm}^{III}(x) = \frac{\zeta_m^2 - k^2}{j\omega\mu\gamma_{nm}} F_{nm} \frac{\cosh \gamma_{nm} [x - (a + 2g + d)]}{\sinh \gamma_{nm} d} \quad (3.20c)$$

Substitution of Eqs. 3.20 into Eqs. 3.19 now yields

$$\sum_{n=-\infty}^{\infty} \sum_{m=0}^{\infty} \frac{\zeta_m^2 - k^2}{\gamma_{nm}} \left[2 A_{nm} \tanh \gamma_{nm} a + (A_{nm} - F_{nm}) \tanh \gamma_{nm} g \right. \\ \left. + (A_{nm} + F_{nm}) \coth \gamma_{nm} g \right] \cos \zeta_m y e^{-j\beta_n z} = 0 \quad (3.21a)$$

$$\sum_{n=-\infty}^{\infty} \sum_{m=0}^{\infty} \frac{\zeta_m^2 - k^2}{\gamma_{nm}} \left[(A_{nm} - F_{nm}) \tanh \gamma_{nm} g - (A_{nm} + F_{nm}) \coth \gamma_{nm} g \right. \\ \left. - 2 F_{nm} \coth \gamma_{nm} d \right] \cos \zeta_m y e^{-j\beta_n z} = 0 \quad (3.21b)$$

Comparison of the preceding two equations shows that they can be equated so that the orthogonal properties of the functions may be used to equate the summands to obtain

$$A_{nm} = - \frac{\coth \gamma_{nm} d + \coth \gamma_{nm} g}{\tanh \gamma_{nm} a + \coth \gamma_{nm} g} F_{nm} \quad (3.22)$$

Substitution of Eq. 3.22 into Eq. 3.21b and use of hyperbolic identities yields

$$\sum_{n=-\infty}^{\infty} \sum_{m=0}^{\infty} \frac{\zeta_m^2 - k^2}{\gamma_{nm}} F_{nm} \left\{ \left[1 + \tanh \gamma_{nm} (a + g) \tanh \gamma_{nm} g \right] \coth \gamma_{nm} d \right. \\ \left. + \tanh \gamma_{nm} (a + g) + \tanh \gamma_{nm} g \right\} \cos \zeta_m y e^{-j\beta_n z} = 0 \quad (3.23)$$

The constant F_{nm} appearing in Eq. 3.23 will now be evaluated by specification of the excitation. Let the outside ladder plane at the q th ladder slot be excited with an axial electric field which is constant across the slot axially. Transversely, the \mathcal{E}_z field must be zero in the ladder plane except in the slot where a cosine variation will be assumed. Expressed mathematically,

$$\mathcal{E}_z(a + 2g, y, z, t) = \begin{cases} E_0 \cos \frac{\pi y}{2b} e^{j(\omega t - \beta_0 pq)}, \\ -b < y < b, pq - \frac{\delta}{2} < z < pq + \frac{\delta}{2} \\ 0, \text{ elsewhere in the rectangle} \\ -c < y < c, pq - \frac{p}{2} < z < pq + \frac{p}{2} \end{cases} \quad (3.24)$$

Since

$$\mathcal{E}_z(a + 2g, y, z, t) = - \sum_{n=-\infty}^{\infty} \sum_{m=0}^{\infty} F_{nm} \cos \left[(2m + 1) \frac{\pi y}{2c} \right] e^{j(\omega t - \beta_n z)} \quad (3.25)$$

then from Eq. 3.24 and Eq. 3.25 it follows from the orthogonality of the functions that

$$\begin{aligned}
 F_{nm} &= -\frac{E_o e^{-j\beta_o pq}}{cp} \int_{pq - \delta/2}^{pq + \delta/2} \int_{-b}^b \cos \frac{\pi y}{2b} \cos \left[(2m+1) \frac{\pi y}{2c} \right] e^{j\beta_n z} dy dz \\
 &= -\frac{E_o}{cp} \frac{4}{\pi} \left\{ \left[\frac{\cos \left[(2m+1) \frac{\pi b}{2c} \right]}{\frac{(2m+1)}{c} + \frac{1}{b}} - \frac{\cos \left[(2m+1) \frac{\pi b}{2c} \right]}{\frac{(2m+1)}{c} - \frac{1}{b}} \right] \right. \\
 &\quad \left. \frac{e^{j\beta_n \delta/2} - e^{-j\beta_n \delta/2}}{2j\beta_n} \right\} \\
 &= E_o \left[\frac{b}{p} \frac{\sin \frac{\beta_n \delta}{2}}{\frac{\beta_n \delta}{2}} \right] \left[\frac{4}{\pi} \frac{1}{\frac{b}{c}} \frac{\cos \left[(2m+1) \frac{\pi b}{2c} \right]}{(2m+1)^2 - \frac{1}{\left(\frac{b}{c}\right)^2}} \right] \quad (3.26)
 \end{aligned}$$

For use in later work two convenient definitions are

$$E'_m = -\frac{4}{\pi} \frac{1}{\frac{b}{c}} \frac{\cos \left[(2m+1) \frac{\pi b}{2c} \right]}{(2m+1)^2 - \left(\frac{1}{\frac{b}{c}}\right)^2} \quad (3.27a)$$

$$E_n = \frac{E_0}{p} \frac{\sin \frac{\beta_n \delta}{2}}{\frac{\beta_n \delta}{2}} \quad (3.27b)$$

so that

$$E_{LM} = \dots E_n E_n E_m \quad (3.27c)$$

For simplification of the notation the following definitions are also useful:

$$\sum_n \equiv \sum_{n=-\infty}^{\infty}, \quad \sum_m \equiv \sum_{m=0}^{\infty}, \quad \sum_{nm} \equiv \sum_n \sum_m \quad (3.27d)$$

In the next section the magnitude of the total nth component of axial electric field at various points in the ladder structure will be required. These expressions will be derived now. From Eqs. 3.25 and 3.27 it follows, using a summation formula of Collin,²² that the magnitude of the nth component of the axial electric field at the center of the outside ladder plane is

$$\begin{aligned}
\left| \mathcal{E}_{zn} (a + 2g, 0, z, t) \right| &= \left| - \sum_m F_{nm} \right| = \left| E_o E_n \sum_m E'_m \right| \\
&= \left| -E_o E_n \frac{4}{\pi} \frac{1}{b} \sum_m \frac{\cos \left[(2m + 1) \frac{\pi b}{2c} \right]}{(2m + 1)^2 - \left(\frac{1}{b} \right)^2} \right| \\
&= \left| -E_o E_n \frac{4}{\pi} \frac{1}{b} \frac{\pi \sin \left[\frac{1}{b} \left(\frac{\pi}{2} - \frac{\pi}{2} \frac{b}{c} \right) \right]}{4 \frac{1}{b} \cos \left(\frac{\pi}{2} \frac{1}{b} \right)} \right| \\
&= \left| -E_o E_n \frac{4}{\pi} \frac{1}{b} \frac{\pi}{4} \frac{b}{c} \frac{\sin \left(\frac{\pi}{2} \frac{1}{b} - \frac{\pi}{2} \right)}{\cos \left(\frac{\pi}{2} \frac{1}{b} \right)} \right| \\
&= \left| E_o E_n \right| \tag{3.28a}
\end{aligned}$$

At the center of the inside ladder plane the magnitude of the field

component is

$$\begin{aligned}
 \left| \mathcal{E}_{zn} (a, 0, z, t) \right| &= \left| \sum_m E_{znm}^I (a) \right| \\
 &= \left| \sum_m -F_{nm} - \sum_m F_{nm} \left(-\frac{A_{nm}}{F_{nm}} - 1 \right) \right| \\
 &= M_n \left| E_o E_n \right| \tag{3.28b}
 \end{aligned}$$

where M_n is the ratio of the magnitude of the field at the inside ladder plane to that at the outside ladder plane and is expressible in a rapidly convergent form by

$$\begin{aligned}
 M_n &= \left| 1 + \sum_m E'_m \left(-\frac{A_{nm}}{F_{nm}} - 1 \right) \right| \\
 &= \left| 1 - \frac{4}{\pi} \frac{1}{\frac{b}{c}} \sum_m \frac{\cos \left[(2m+1) \frac{\pi b}{2c} \right]}{(2m+1)^2 - \left(\frac{1}{\frac{b}{c}} \right)^2} \frac{\coth \gamma_{nm} d - \tanh \gamma_{nm} a}{\coth \gamma_{nm} g + \tanh \gamma_{nm} a} \right| \tag{3.28c}
 \end{aligned}$$

At the center of the ladder structure it is found that

$$\begin{aligned}
 \left| \varepsilon_{zn} (0,0,z,t) \right| &= \left| \sum_m E_{znm}^I(0) \right| = \left| \sum_m A_{nm} \operatorname{sech} \gamma_{nm} a \right| \\
 &= \left| \sum_m -F_{nm} \left(-\frac{A_{nm}}{F_{nm}} \right) \operatorname{sech} \gamma_{nm} a \right| \\
 &= \left| E_o E_n \right| N_n \tag{3.28d}
 \end{aligned}$$

where N_n is the ratio of the magnitude of the field at the center of the structure to that at the outside ladder plane and is expressible in a convenient form by

$$N_n = \frac{4}{\pi} \frac{1}{\frac{b}{c}} \left| \sum_m \frac{\cos \left[(2m+1) \frac{\pi b}{2c} \right]}{(2m+1)^2 - \left(\frac{1}{\frac{b}{c}} \right)^2} \frac{\coth \gamma_{nm} d + \coth \gamma_{nm} g}{\tanh \gamma_{nm} a + \coth \gamma_{nm} g} \operatorname{sech} \gamma_{nm} a \right| \tag{3.28e}$$

The equation for Ω_n , the ratio of the nth component of axial electric

field midway between the two outer ladders to the field at the outside ladder, is found from

$$\begin{aligned}
 \left| \mathcal{E}_{zn}(a+g, 0, z, t) \right| &= \left| \sum_m E_{znm}^{II} (a+g) \right| \\
 &= \left| \frac{1}{2} \sum_m -F_{nm} \left(-\frac{A_{nm}}{F_{nm}} + 1 \right) \operatorname{sech} \gamma_{nm} g \right| \\
 &= \left| E_o E_n \right| \Omega_n \tag{3.28f}
 \end{aligned}$$

so that

$$\Omega_n = \frac{2}{\pi} \frac{1}{\frac{b}{c}} \left| \sum_m \frac{\cos \left[(2m+1) \frac{\pi b}{2c} \right]}{(2m+1)^2 - \left(\frac{1}{\frac{b}{c}} \right)^2} \left(\frac{\coth \gamma_{nm} d + \coth \gamma_{nm} g}{\tanh \gamma_{nm} a + \coth \gamma_{nm} g} + 1 \right) \operatorname{sech} \gamma_{nm} g \right| \tag{3.28g}$$

The quantity $\Pi_n(\theta)$ which is the ratio of the magnitude of the nth component of the axial electric field at a distance θd , $0 \leq \theta \leq 1$,

from the outside ladder to that at the outside ladder, is found as follows:

$$\begin{aligned}
 \left| \varepsilon_{zn}(a+2g+\theta d, 0, z, t) \right| &= \left| \sum_m E_{znm}^{\text{III}}(a+2g+\theta d) \right| \\
 &= \left| \sum_m -F_{nm} \frac{\sinh \left[\gamma_{nm} d(1 - \theta) \right]}{\sinh \gamma_{nm} d} \right| \\
 &= \left| E_o E_n \right| \Pi_n(\theta) \tag{3.28h}
 \end{aligned}$$

when

$$\Pi_n(\theta) = \frac{4}{\pi} \frac{1}{\frac{b}{c}} \left| \sum_m - \frac{\cos \left[(2m+1) \frac{\pi b}{2c} \right]}{(2m+1)^2 \left(\frac{1}{\frac{b}{c}} \right)^2} \frac{\sinh \left[\gamma_{nm} d(1 - \theta) \right]}{\sinh \gamma_{nm} d} \right| \tag{3.28i}$$

Reference to Eq. 3.28a shows that $1 \geq \Pi_n(\theta) \geq 0$.

The phase constant β_o can now be obtained from Eq. 3.23. As is common in this type of analysis, we are unable to match the fields throughout the entire ladder region and so we shall set $y = 0$ and $z = pq$, q an integer, and match the fields at the center of each slot. With this done and with the definitions that

$$k_c = \frac{2\pi}{\lambda_c} = \frac{\pi}{2c}$$

and

$$L_{nm} = \left\{ 1 + \tanh \left[\frac{\pi}{2} \frac{Y_{nm}}{k_c} \left(\frac{a}{c} + \frac{g}{c} \right) \right] \tanh \left[\frac{\pi}{2} \frac{Y_{nm}}{k_c} \frac{g}{c} \right] \right\} \coth \left[\frac{\pi}{2} \frac{Y_{nm}}{k_c} \frac{d}{c} \right] \\ + \tanh \left[\frac{\pi}{2} \frac{Y_{nm}}{k_c} \left(\frac{a}{c} + \frac{g}{c} \right) \right] + \tanh \left[\frac{\pi}{2} \frac{Y_{nm}}{k_c} \frac{g}{c} \right] \quad (3.29)$$

Equation 3.23 yields the determinantal equation for β_0 :

$$\sum_{nm} \frac{(2m+1)^2 - \left(\frac{k}{k_c}\right)^2}{(2m+1)^2 - \frac{1}{\left(\frac{b}{c}\right)^2}} \frac{\sin \left[\frac{\pi}{2} \frac{\delta}{p} \frac{\beta_n}{k_c} \frac{p}{2c} \right]}{\left[\frac{\pi}{2} \frac{\delta}{p} \frac{\beta_n}{k_c} \frac{p}{2c} \right]} \frac{\cos \left[(2m+1) \frac{\pi b}{2c} \right]}{\frac{Y_{nm}}{k_c}} L_{nm} = 0 \quad (3.30)$$

where

$$\frac{\beta_n}{k_c} = \frac{\beta_0}{k_c} + \frac{2n}{\frac{p}{2c}} \quad (3.31)$$

and

$$\left(\frac{Y_{nm}}{k_c} \right)^2 = (2m+1)^2 + \left(\frac{\beta_n}{k_c} \right)^2 - \left(\frac{k}{k_c} \right)^2 \quad (3.32)$$

Values of β_0/k_c and corresponding values of k/k_c have been obtained from Eq. 3.30 for a number of special cases using the Burroughs Datatron 205 digital computer. The results for the zero-pitch (current-sheet) approximation were obtained previously and appeared in earlier reports.^{23,24} The curves shown on the ω - β diagrams in Figs. 5 and 6 give a good indication of the effect on the dispersion of changes in pitch and ladder-plane spacing. It can be seen that a larger pitch or ladder plane spacing causes the curve to shift upward. The information about the phase characteristics of the coupled ladder circuit will be useful in the design of the tube.

Another item of interest, especially for theoretical considerations of power output, is the impedance characteristics. This topic will be the subject of the next section.

3.2 Impedance Characteristics

In the previous section the theoretical propagation characteristics of coupled ladder circuits were derived. This section will derive the impedance expression and present the results graphically. The interaction impedance gives an index of the strength of one of the space harmonics of the axial electric field with reference to the total power in the mode of interest. Let K_n , the axial interaction impedance of the n th space harmonic at the top ladder be defined as follows:¹⁸

$$K_n (a + 2g) = \frac{|\mathcal{E}_{zn} (a + 2g, 0, z, t)|^2}{2\beta_n^2 W_{av}} \quad (3.33)$$

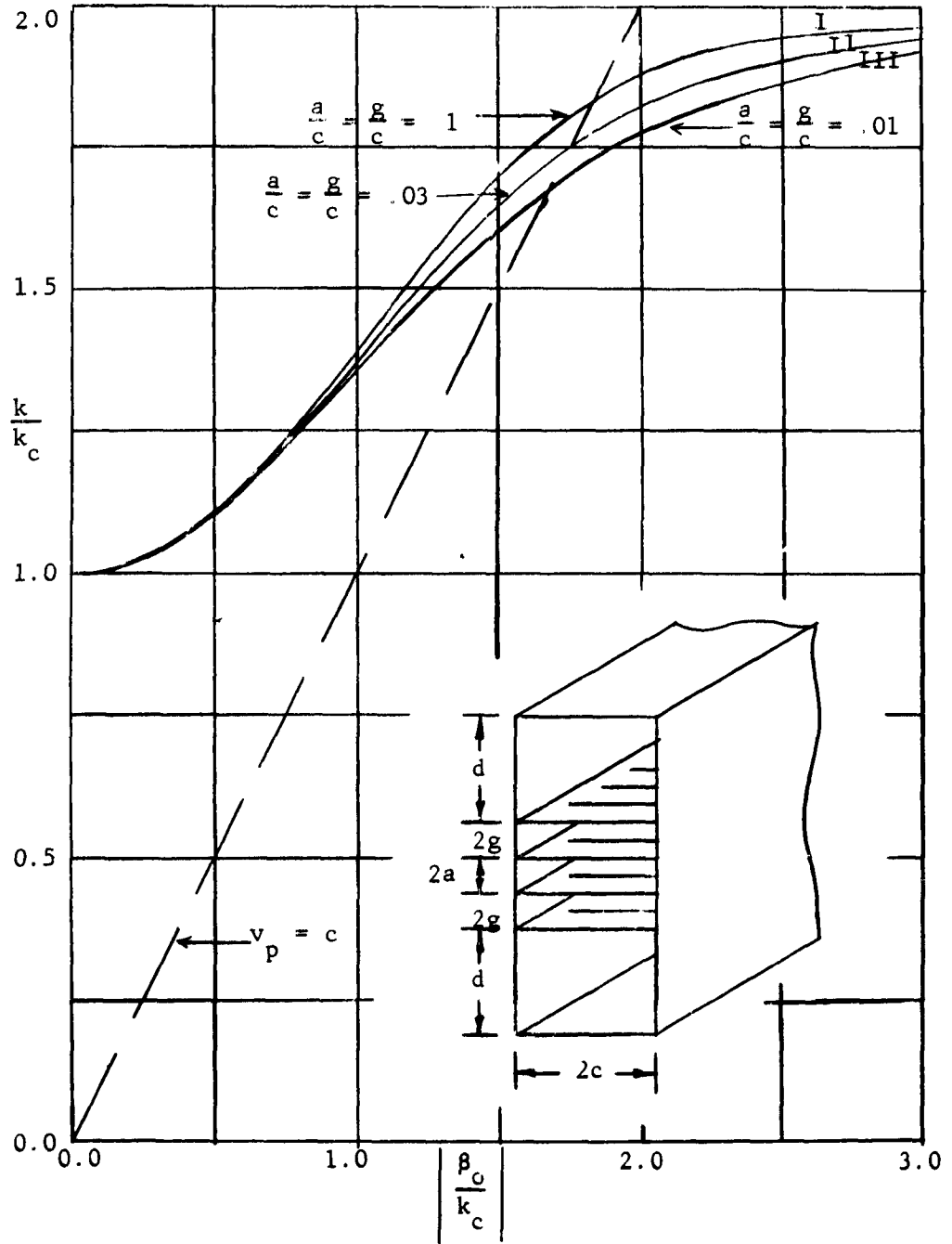


Fig. 5. Propagation constants for four coupled ladder planes in 2:1 waveguide. The curves were computed for values of $a/c = g/c = 0.01, 0.03$ and 0.10 with $p/2c = 0.2$, $b/c = 0.5$, and $\delta/p = 0.5$.

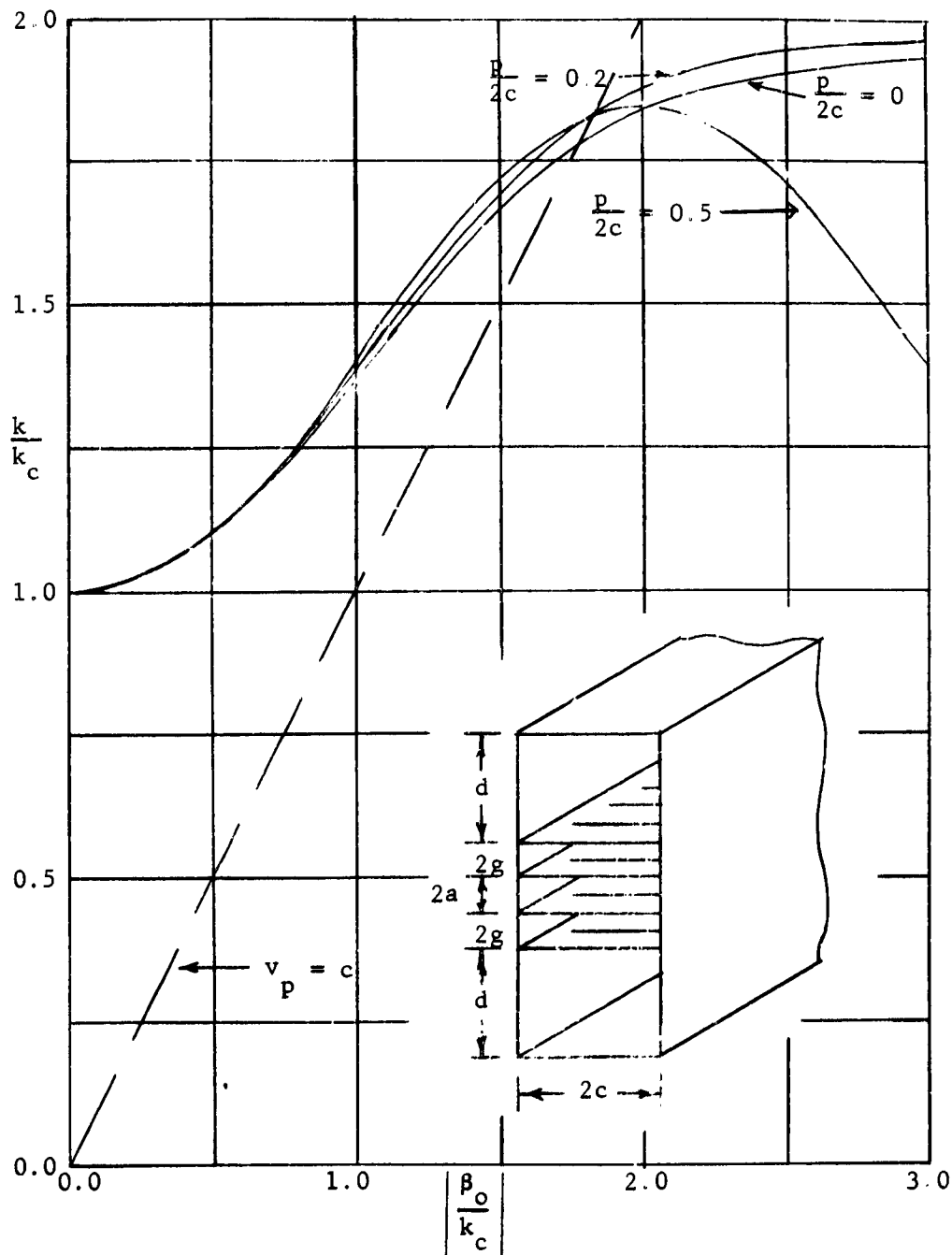


Fig. 6. Propagation constants for four coupled ladder planes in 2:1 waveguide. The curves were computed for values of $p/2c = 0, 0.2$ and 0.5 with $a/c = g/c = 0.10$, $b/c = 0.5$, and $\delta/p = 0.5$.

where W_{av} , the total time-average power carried by the mode, is expressible in terms of the fields by the Poynting theorem.

$$W_{av} = \int_S \bar{P} \cdot \overline{dS} = 4 \int_0^{a+2g+d} \int_0^c P_z dydx \quad (3.34)$$

Using the complex forms of the field vectors P_z may be expressed

$$P_z = \frac{1}{2} \operatorname{Re} (\bar{E} \times \bar{H}^*) \cdot \hat{z} = \frac{1}{2} \operatorname{Re} \epsilon_x \mathcal{H}_y^* = \frac{1}{2} \operatorname{Re} \sum_{nm} \epsilon_{xnm} \sum_{sr} \mathcal{H}_{ysr}^* \quad (3.35)$$

Use of Eqs. 3.7, 3.16, and 3.17 gives ϵ_{xnm} and \mathcal{H}_{ysr}^*

$$\epsilon_{xnm} = j \frac{\beta_n}{2 \gamma_{nm}} \frac{\partial \mathcal{E}_{znm}}{\partial x} \quad (3.36)$$

$$\mathcal{H}_{ysr}^* = j \frac{\zeta_r^2 - k^2}{\omega \mu \gamma_{sr}} \frac{\partial \mathcal{E}_{zsr}^*}{\partial x}$$

From Eq. 3.35 it follows that

$$\begin{aligned}
 P_z &= - \frac{1}{2\omega\mu} \operatorname{Re} \sum_{nmsr} \frac{\beta_n}{\gamma_{nm}} \frac{\zeta_r^2 - k^2}{\gamma_{sr}^2} \frac{\partial \mathcal{E}_{znm}}{\partial x} \frac{\partial \mathcal{E}_{zsr}^*}{\partial x} \\
 &= - \frac{1}{2\omega\mu} \operatorname{Re} \sum_{nmsr} \frac{\beta_n}{\gamma_{nm}} \frac{\zeta_r^2 - k^2}{\gamma_{sr}^2} \frac{d\mathcal{E}_{znm}}{dx} \frac{d\mathcal{E}_{zsr}}{dx} \\
 &\quad \cos \zeta_m y \cos \zeta_r y e^{j(\beta_s - \beta_n)z} \\
 &= - \frac{1}{4\omega\mu} \sum_{nmsr} \frac{\beta_n}{\gamma_{nm}} \frac{\zeta_r^2 - k^2}{\gamma_{sr}^2} \frac{d\mathcal{E}_{znm}}{dx} \frac{d\mathcal{E}_{zsr}}{dx} \\
 &\quad \left\{ \cos \left[(r + m + 1) \frac{\pi}{c} y \right] + \cos \left[(r - m) \frac{\pi}{c} y \right] \right\} \cos \left[\frac{2\pi}{p} (s - n) z \right] \quad (3.37)
 \end{aligned}$$

The average power must be independent of z , so Eq. 3.37 may be averaged over z

$$\frac{1}{p} \int_{p(q - \frac{1}{2})}^{p(q + \frac{1}{2})} \cos \left[\frac{2\pi}{p} (s - n) z \right] dz = \delta_{sn} \quad (3.38)$$

where δ_{sn} is the Kronecker delta defined to be unity for like indices and zero if the indices are different. Thus, $s = n$.

Let the y -integration now be performed to yield

$$\int_0^c \left\{ \cos \left[(r + m + 1) \frac{\pi}{c} y \right] + \cos \left[(r - m) \frac{\pi}{c} y \right] \right\} dy = \delta_{rm} c \quad (3.39)$$

so that $r = m$ also. Therefore, Eq. 3.37 simplifies to

$$P_z = -\frac{c}{4\omega\mu} \sum_{nm} \frac{\beta_n (\zeta_m^2 - k^2)}{\gamma_{nm}^4} \left(\frac{dE_{znm}}{dx} \right)^2 \quad (3.40)$$

The average power can now be found from Eq. 3.34.

$$W_{av} = \frac{c}{2\omega\mu} \sum_{nm} \frac{\beta_n (k^2 - \zeta_m^2)}{\gamma_{nm}^3} F_{nm}^2 \left\{ \frac{2}{\gamma_{nm} F_{nm}^2} \int_0^a \left(\frac{dE_{znm}^I}{dx} \right)^2 dx \right. \\ \left. + \frac{2}{\gamma_{nm} F_{nm}^2} \int_a^{a+2g} \left(\frac{dE_{znm}^{II}}{dx} \right)^2 dx + \frac{2}{\gamma_{nm} F_{nm}^2} \int_{a+2g}^{a+2g+d} \left(\frac{dE_{znm}^{III}}{dx} \right)^2 dx \right\} \quad (3.41)$$

Let the quantity in the braces in Eq. 3.41 be known as $S_{nm} = S_{nm}^I + S_{nm}^{II} + S_{nm}^{III}$. Using Eqs. 3.11, we can now find S_{nm} . The following formulas

will be useful:

$$2\gamma_{nm} \int \sinh^2 \gamma_{nm} (x - \phi) dx = \sinh \gamma_{nm} (x - \phi) \cosh \gamma_{nm} (x - \phi) - \gamma_{nm} (x - \phi) \quad (3.42a)$$

$$2\gamma_{nm} \int \sinh \gamma_{nm} (x - \phi) \cosh \gamma_{nm} (x - \phi) dx = \sinh^2 \gamma_{nm} (x - \phi) \quad (3.42b)$$

$$2\gamma_{nm} \int \cosh^2 \gamma_{nm} (x - \phi) dx = \sinh \gamma_{nm} (x - \phi) \cosh \gamma_{nm} (x - \phi) + \gamma_{nm} (x - \phi) \quad (3.42c)$$

Then, with the definition using Eq. 2.22 that

$$T_{nm} = - \frac{A_{nm}}{F_{nm}} = \frac{\coth \gamma_{nm} d + \coth \gamma_{nm} g}{\tanh \gamma_{nm} a + \coth \gamma_{nm} g} \quad (3.42d)$$

it follows from Eqs. 3.11 and 3.42 that

$$\begin{aligned} S_{nm}^I &= \frac{2\gamma_{nm}}{F_{nm}^2} \int_0^a A_{nm}^2 \frac{\sinh^2 \gamma_{nm} x}{\cosh^2 \gamma_{nm} a} dx \\ &= T_{nm}^2 \left\{ \tanh \gamma_{nm} a - \frac{\gamma_{nm} a}{\cosh^2 \gamma_{nm} a} \right\} \quad (3.43a) \end{aligned}$$

and also, with Eqs. 3.18

$$\begin{aligned}
 S_{nm}^{II} &= \frac{2\gamma_{nm}}{F_{nm}^2} \int_a^{a+2g} \left\{ C_{nm}^2 \frac{\sinh^2 \gamma_{nm} [x - (a+g)]}{\cosh^2 \gamma_{nm} g} \right. \\
 &\quad + 2C_{nm} C'_{nm} \frac{\sinh \gamma_{nm} [x - (a+g)] \cosh \gamma_{nm} [x - (a+g)]}{\sinh \gamma_{nm} g \cosh \gamma_{nm} g} \\
 &\quad \left. + C'_{nm}{}^2 \frac{\cosh^2 \gamma_{nm} [x - (a+g)]}{\sinh^2 \gamma_{nm} g} \right\} dx \\
 &= \frac{1}{2} (T_{nm} + 1)^2 \left\{ \tanh \gamma_{nm} g - \frac{\gamma_{nm} g}{\cosh^2 \gamma_{nm} g} \right\} \\
 &\quad + \frac{1}{2} \frac{(T_{nm} - 1)^2}{\tanh^2 \gamma_{nm} g} \left\{ \tanh \gamma_{nm} g + \frac{\gamma_{nm} g}{\cosh^2 \gamma_{nm} g} \right\} \quad (3.43b)
 \end{aligned}$$

and finally that

$$S_{nm}^{III} = \frac{2\gamma_{nm}}{F_{nm}^2} \int_{a+2g}^{a+2g+d} \frac{\cosh^2 \gamma_{nm} [x - (a+2g+d)]}{\sinh^2 \gamma_{nm} d} dx = \coth \gamma_{nm} d + \frac{\gamma_{nm} d}{\sinh^2 \gamma_{nm} d} \quad (3.43c)$$

Therefore, with T_{nm} given by Eq. 3.42d one may write

$$\begin{aligned}
 S_{nm} = & T_{nm}^2 \left\{ \tanh \gamma_{nm} a - \gamma_{nm} a \operatorname{sech}^2 \gamma_{nm} a \right\} \\
 & + \frac{1}{2} (T_{nm} + 1)^2 \left\{ \tanh \gamma_{nm} g - \gamma_{nm} g \operatorname{sech}^2 \gamma_{nm} g \right\} \\
 & + \frac{1}{2} \frac{(T_{nm} - 1)^2}{\tanh^2 \gamma_{nm} g} \left\{ \tanh \gamma_{nm} g + \gamma_{nm} g \operatorname{sech}^2 \gamma_{nm} g \right\} \\
 & + \coth \gamma_{nm} d + \gamma_{nm} d \operatorname{csch}^2 \gamma_{nm} d
 \end{aligned} \tag{3.44}$$

The power flow, with Eqs. 3.27 and 3.41, becomes

$$W_{av} = \frac{cE_o^2}{2\omega\mu} \sum_{nm} \frac{\beta_n (k^2 - \zeta_m^2)}{\gamma_{nm}^3} E_n^2 E_m'^2 S_{nm} \tag{3.45}$$

It is convenient to normalize Eq. 3.45 to the cutoff wave number k_c .

With $\eta_0 = (\mu/\epsilon)^{1/2} \approx 120\pi$, the the average power flow may be written

$$W_{av} = \frac{\pi}{4} \frac{E_0^2}{\eta_0 k_c^2} \frac{1}{\frac{k}{k_c}} \sum_{nm} \frac{\left(\frac{k}{k_c}\right)^2 - (2m+1)^2}{\left(\frac{\gamma_{nm}}{k_c}\right)^3} \frac{\beta_n}{k_c} E_n^2 E_m'^2 S_{nm} \quad (3.46)$$

where β_0/k_c is found from Eq. 3.30.

Equations 3.28a, 3.33, and 3.46 can be used to find the interaction impedance of the ν th harmonic at the center of the outside ladder plane

$$K_\nu(a+2g) = \eta_0 \frac{k}{k_c} \frac{\left(\frac{\delta}{p}\right)^2 \frac{\sin^2 \left[\frac{\pi}{2} \frac{\beta_\nu}{k_c} \frac{p}{2c} \frac{\delta}{p} \right]}{\left(\frac{\pi}{2} \frac{\beta_\nu}{k_c} \frac{p}{2c} \frac{\delta}{p} \right)^2} \frac{1}{\frac{\pi}{2} \left(\frac{\beta_\nu}{k_c}\right)^2 \sum_{nm} \frac{\left(\frac{k}{k_c}\right)^2 - (2m+1)^2}{\left(\frac{\gamma_{nm}}{k_c}\right)^3} \frac{\beta_n}{k_c} E_n^2 E_m'^2 S_{nm}} \quad (3.47)$$

The ratio of the backward-wave impedance ($\nu = -1$) to the forward-wave

impedance ($\nu = 0$) can also be found. From Eq. 3.47

$$\frac{K_{-1}(a+2g)}{K_0(a+2g)} = \frac{\sin^2 \left[\left(\pi - \frac{\pi\beta_0}{2k_c} \frac{p}{2c} \right) \frac{\delta}{p} \right]}{\sin^2 \left[\frac{\pi}{2} \frac{\beta_0}{k_c} \frac{p}{2c} \frac{\delta}{p} \right]} \left[\frac{\frac{\pi}{2} \frac{\beta_0}{k_c} \frac{p}{2c}}{\pi - \frac{\pi}{2} \frac{\beta_0}{k_c} \frac{p}{2c}} \right]^4 \quad (3.48)$$

Considering the case where the rung width of the ladders is equal to the slot width, $\delta/p = 1/2$, we obtain

$$K_{-1}(a+2g) = K_0(a+2g) \frac{\cot^2 \left[\frac{\pi}{4} \frac{\beta_0}{k_c} \frac{p}{2c} \right]}{\left[\frac{2}{\frac{\beta_0}{k_c} \frac{p}{2c} - 1} \right]^4} \quad (3.49)$$

Numerical values for $K_0(a+2g)$ and $K_{-1}(a+2g)$ have been obtained on the Datatron 205 digital computer and curves are presented in Figs. 7, 8, 9, and 10 for two values of pitch and for three spacing distances. The backward-wave impedance is highest for large pitch (corresponds to high voltage) and small spacing (very little current):

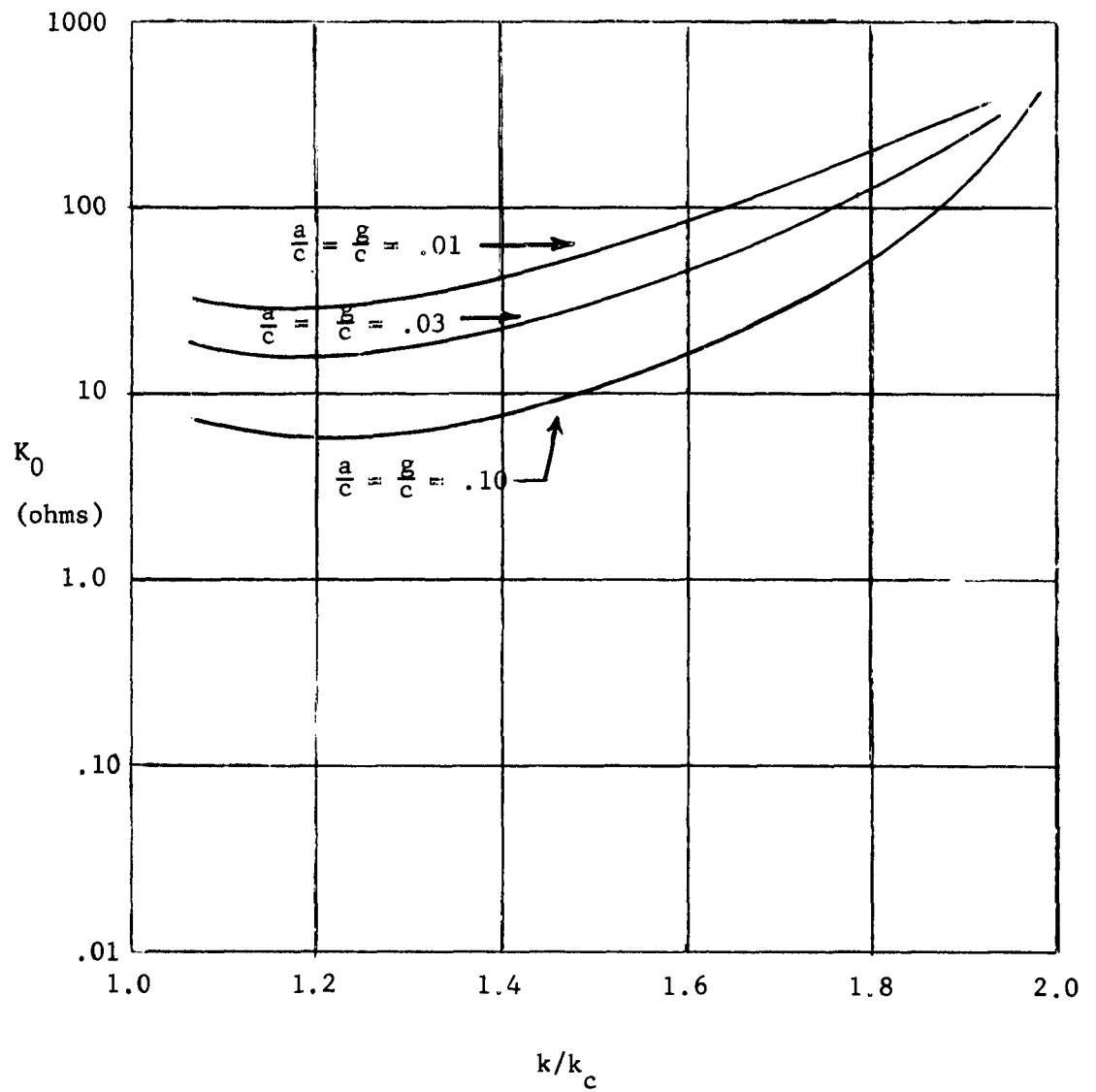


Fig. 7. Forward-wave impedance at the center of the outer ladder for four coupled ladders in 2:1 waveguide. The curves were computed for values of $a/c = g/c = 0.01, 0.03$ and 0.10 with $p/2c = 0.2$, $b/c = 0.5$, and $\delta/p = 0.5$.

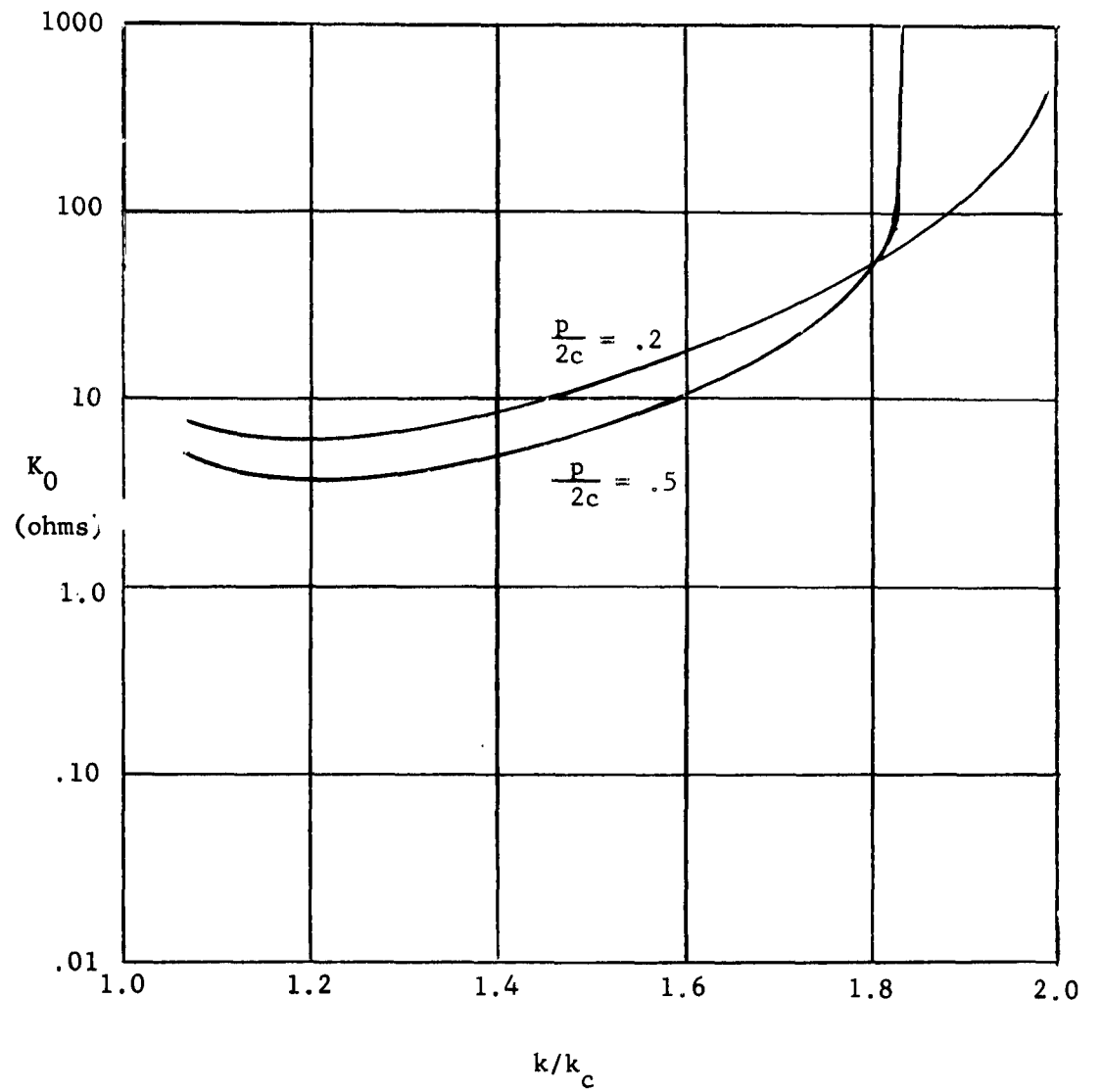


Fig. 8. Forward-wave impedance at the center of the outer ladder for four coupled ladders in 2:1 waveguide. The curves were computed for values of $p/2c = 0.2$ and 0.5 with $a/c = g/c = 0.10$, $b/c = 0.5$, and $\delta/p = 0.5$.

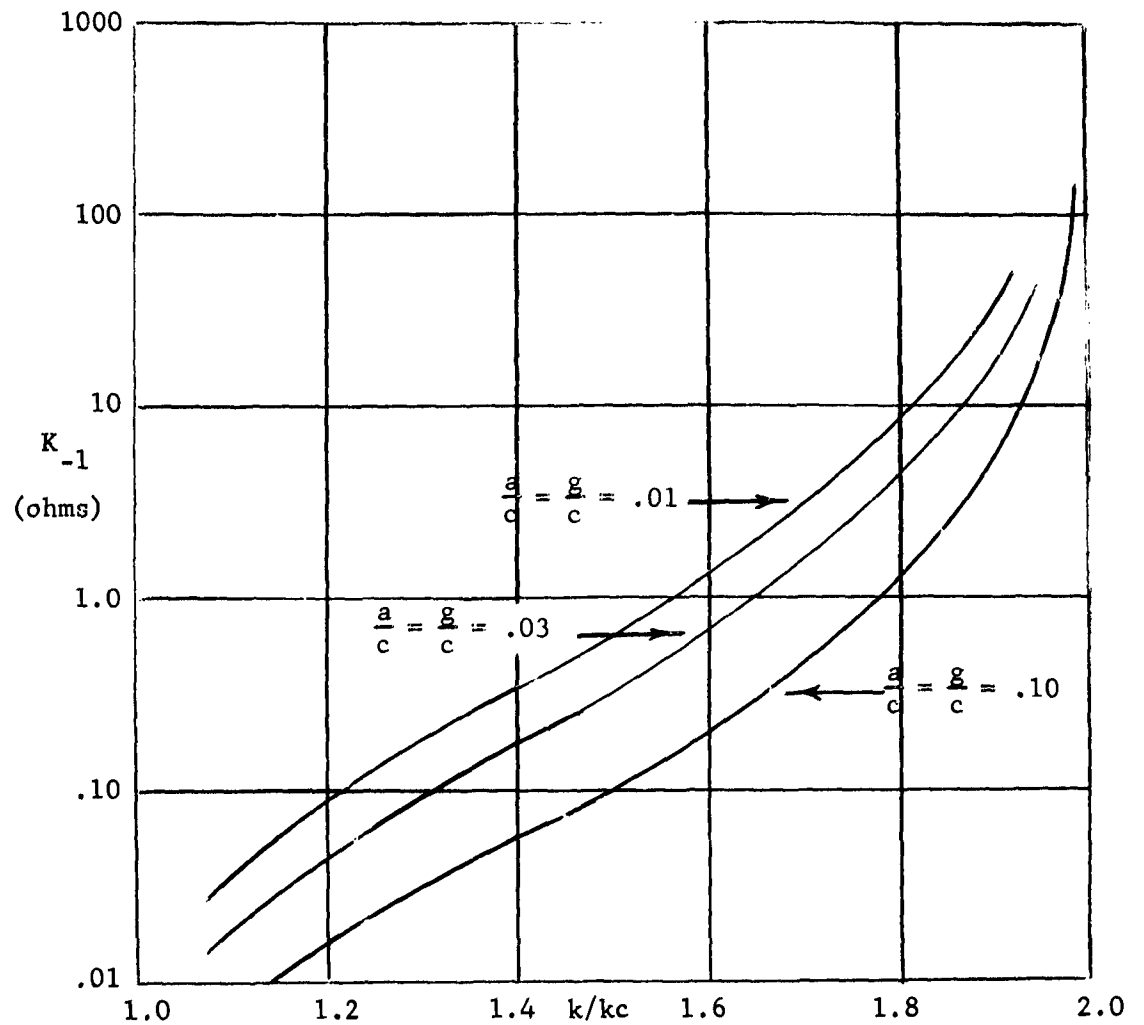


Fig. 9. Backward-wave impedance at the center of the outer ladder for four coupled ladders in 2:1 waveguide. The curves were computed for values of $a/c = g/c = 0.01$, 0.03 and 0.10 with $p/2c = 0.2$, $b/c = 0.5$, and $\delta/p = 0.5$.

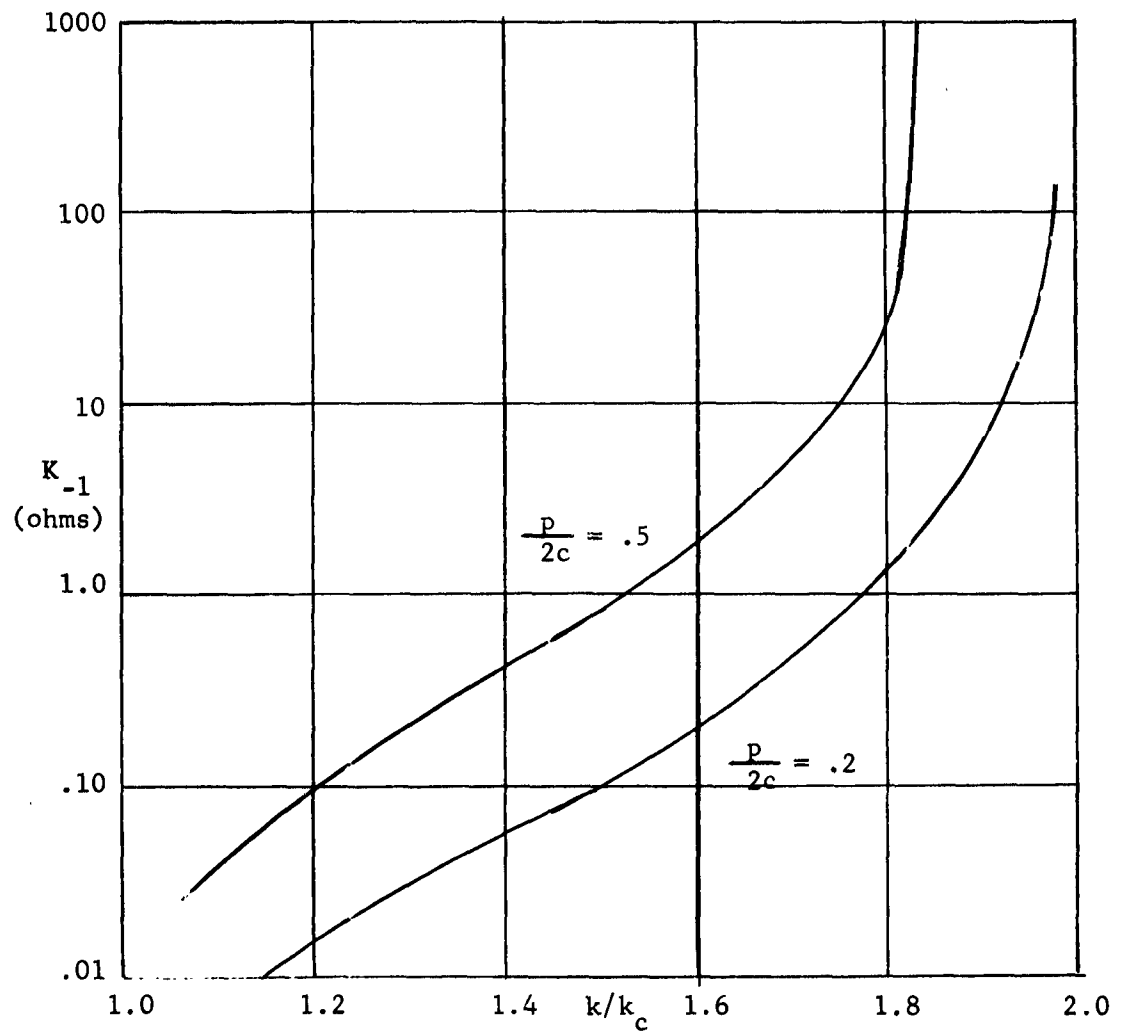


Fig. 10. Backward-wave impedance at the center of the outer ladder for four coupled ladders in 2:1 waveguide. The curves were computed for values of $p/2c = 0.2$ and 0.5 with $a/c = g/c = 0.10$, $b/c = 0.5$ and $\delta/p = 0.5$.

A more complete analysis is needed, one that will show the average impedance presented to the cross-section of the electron stream. An average value of $I_o K_n$ for use in Pierce's gain parameter C^3 (see Eq. 2.5b) will be determined by using the equation

$$(I_o K_n)_{av} = 4K_n(a+2g) \int_0^{a+2g+d} \int_0^c J(x,y) \frac{K_n(x,y)}{K_n(a+2g)} dy dx \quad (3.50)$$

Since there will be a distance s away from the ladder planes where due to interception there is essentially no current the current density in the (rectangular) beam of sides $2q$, $2r$ can be approximated with the discontinuous function

$$J(x,y) = J_o \text{ inside the rectangles}$$

$$0 < x < (a - s), (a + s) < x < (a + 2g - s)$$

$$(a + 2g + s) < x < q$$

$$-r < y < r \quad (3.51)$$

and $J(x,y)$ is zero otherwise. The impedance function can also be approximated. Since $K_n(x,y)$ varies as the square of the magnitude of the axial electric field, the variation of K_n with y is

$$K_n(y) = \cos^2 \frac{\pi y}{2b} \quad (3.52)$$

The variation of K_n with x is also found from the axial electric field functions. Since the n th component of axial electric field depends in a rather involved way upon x , $E_n(x)$ will be computed at selected points and these points will be connected with the hyperbolic curves shown in Fig. 11. The values of M_n , N_n , Ω_n , Π_n are given by Eqs. 3.28. The normalized impedance functions for use in Eq. 3.50 are

Region I:

$$\frac{K_n^I(x)}{K_n(a+2g)} = \left\{ N_n \cosh \left[\left(\frac{1}{a} \cosh^{-1} \frac{M_n}{N_n} \right) x \right] \right\}^2 \quad (3.53a)$$

Region II:

$$\begin{aligned} \frac{K_n^{II}(x)}{K_n(a+2g)} = & \left\{ \Omega_n \cosh \left[- \left(\frac{1}{g} \cosh^{-1} \frac{M_n + 1}{2\Omega_n} \right) [x - (a+g)] \right] \right. \\ & \left. + \Omega_n \sinh \left[- \left(\frac{1}{g} \sinh^{-1} \frac{M_n - 1}{2\Omega_n} \right) [x - (a+g)] \right] \right\}^2 \end{aligned} \quad (3.53b)$$

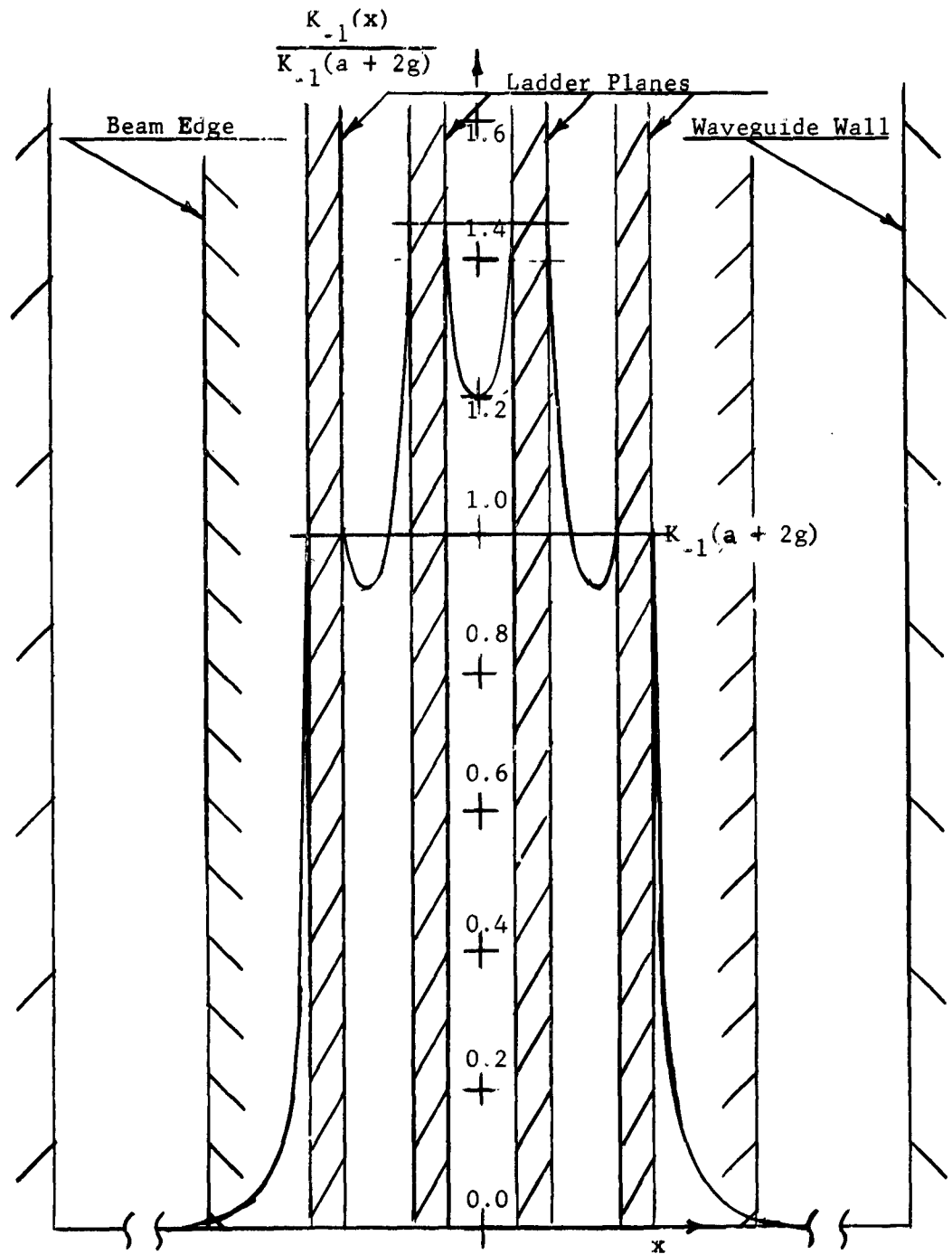


Fig. 11. Variation of interaction impedance across the beam at the center of the ladder planes for the backward wave. The beam diameter is 0.116" and the ladder plane separation is 0.010".

Region III:

$$\frac{K_n^{III}(x)}{K_n(a+2g)} = \left\{ \frac{1}{\sinh \tau} \sinh \left(\frac{\tau}{d} [x - (a+2g+d)] \right) \right\}^2 \quad (3.53c)$$

where τ is found from θ (see Eq. 3.28i) through the relationship

$$\sinh [\tau(1 - \theta)] = \Pi_n(\theta) \sinh \tau \quad (3.54a)$$

For large τ Eq. 3.54a becomes

$$\tau \approx \frac{1}{\theta} \ln \frac{1}{\Pi_n(\theta)} \quad (3.54b)$$

From Eqs. 3.50, 3.51, and 3.52 it follows that

$$\begin{aligned} \int_0^c J(x,y) \frac{K_n(x,y)}{K_n(a+2g)} dy &= J(x) \frac{K_n(x)}{K_n(a+2g)} \int_0^r \cos^2 \left(\frac{\pi y}{2b} \right) dy \\ &= rJ(x) \frac{K_n(x)}{K_n(a+2g)} \left[\frac{1}{2} + \frac{1}{2} \frac{\sin \frac{\pi r}{b}}{\frac{\pi r}{b}} \right] \quad (3.55) \end{aligned}$$

The final evaluation of $(I_o K_n)_{av}$ using Eq. 3.50 depends only on the evaluation by Eq. 3.42 of the integrals of the expressions given by Eqs. 3.53. Then, with $q = \pi r/4$ for a round beam of radius r Eq. 3.50 yields

$$(I_o K_n)_{av} = \pi r^2 J_o K_n (a+2g) \left[\frac{1}{2} + \frac{1}{2} \frac{\sin \frac{\pi r}{b}}{\frac{\pi r}{b}} \right] \sigma_n \quad (3.56)$$

where the reduction factor²⁵

$$\sigma_n = \frac{1}{\frac{\pi r}{4}} \left(\sigma_n^I + \sigma_n^{II} + \sigma_n^{III} \right) \quad (3.57a)$$

is found from

$$\sigma_n^J = \int_0^{a-s} \frac{K_n^I(x)}{K_n(a+2g)} dx \quad (3.57b)$$

$$\sigma_n^{II} = \int_{a+s}^{a+2g-s} \frac{K_n^{II}(x)}{K_n(a+2g)} dx \quad (3.57c)$$

$$\sigma_n^{III} = \int_{a+2g+s}^{\pi r/4} \frac{K_n^{III}(x)}{K_n(a+2g)} dx \quad (3.57d)$$

The equations for the theoretical propagation constant and impedance parameter are derived in Section III. Curves of these parameters for various pitches and ladder plane spacings have been presented to provide design information.

IV. DISCUSSION OF RESULTS AND CONCLUSIONS

The theoretical propagation and impedance characteristics of four closely-spaced ladder planes in a waveguide have been found and curves have been presented to show the results graphically.

In Section II, a general discussion of the theory of backward-wave oscillators was given. In Section III, the propagation and impedance equations for four coupled ladders in a waveguide were derived and solved. Curves were presented for phase shift versus frequency and interaction impedance versus frequency for both the fundamental forward- and backward-wave modes for various values of pitch and ladder plane spacing. Larger values of pitch or ladder plane spacing increase the frequency corresponding to a given phase shift. The backward-wave impedance is highest for large values of pitch and small values of ladder plane spacing.

On the basis of this study a ladder-type backward-wave oscillator appears to be feasible at millimeter wavelengths. Future plans include the construction and test of a 40 kMc oscillator using a coupled-ladder circuit.

REFERENCES

1. R. Kompfner and N. T. Williams, "Backward-Wave Tubes," Proc. IRE, Vol. 41, pp. 1602-1611, November 1953.
2. R. W. Grow, D. A. Dunn, J. W. McLaughlin, and R. P. Lagerstrom, "A 20 to 40-KMC Backward-Wave Oscillator," IRE Transactions on Electron Devices, Vol. ED-5, pp. 152-156, July 1958.
3. J. L. Putz and G. C. Van Hoven, "Use of Multiple Helix Circuits in 100 Watt CW Traveling-Wave Amplifiers," IRE Wescon Record 1947, Vol. I, Part 3, pp. 138-142.
4. A. Karp, "Traveling-Wave Tube Experiments at Millimeter Wavelengths With a New, Easily Built, Space Harmonic Circuit," Proc. IRE, Vol. 43, pp. 41-46, January 1955.
5. A. Karp, "Backward-Wave Oscillator Experiments at 100 to 200 Kilomegacycles," Proc. IRE, Vol. 45, pp. 496-503, April 1957.
6. Y. Ta and G. Convert, Electron Tubes at Millimeter and Submillimeter Wavelengths, Compagnie Générale de Télégraphie Sans Fil, Paris, France, October 13, 1961.
7. R. M. White, C. K. Birdsall, and R. W. Grow, "Multiple Ladder Circuits for Millimeter Wavelength Traveling Wave Tubes." Proc. of the Symposium on Millimeter Waves, Polytechnic Institute of Brooklyn, March 31, April 1, 2, 1959, pp. 367-402.
8. E. A. Ash, "A New Type of Slow Wave Structure for Millimetre Wavelengths," J.I.E.E., 105 B, 1958, Suppl. 11.
9. E. A. Ash and A. C. Studd, "A Planar Slow Wave Structure for Millimetre Wave Generation," Microwave Tubes, Proc. of the International Congress, Munich, pp. 292-294, New York, Academic Press, 1961.
10. E. A. Ash, "A Note on Impedance and Saturation Power of a Multiple Ladder Array at Millimetre Wavelengths," Journal of Electronics and Control, Vol. X, First Series, pp. 39-43, January 1961.
11. J. R. Pierce, Traveling-Wave Tubes, Princeton, D. Van Nostrand Company, Inc., 1950.
12. D. A. Watkins and E. A. Ash, "The Helix as a Backward-Wave Structure," Journal of Applied Physics, Vol. 25, No. 6, pp. 732-790, June 1954.
13. H. R. Johnson, "Backward-Wave Oscillators," Proc. IRE, Vol. 43, pp. 684-697, June 1955.

14. L. R. Walker, "Starting Currents in the Backward-Wave Oscillator," Journal of Applied Physics, Vol. 24, No. 7, pp. 854-859, July 1953.
15. R. D. Weglein, "Backward-Wave Oscillator Starting Conditions," IRE Transactions on Electron Devices, Vol. ED-4, pp. 177-179, April 1957.
16. R. G. E. Hutter, Beam and Wave Electronics in Microwave Tubes, Princeton, D. Van Nostrand Company, Inc., 1960.
17. H. Heffner, "Analysis of the Backward-Wave Traveling-Wave Tube," Proc. IRE, Vol. 42, pp. 930-937, June 1954.
18. D. A. Watkins, Topics in Electromagnetic Theory, New York, John Wiley and Sons, Inc., 1958.
19. C. C. Johnson, Field and Wave Dynamics, Textbook in preparation at University of Utah.
20. S. Ramo and J. R. Whinnery, Fields and Waves in Modern Radio, Second Edition, New York, John Wiley and Sons, Inc., 1959.
21. W. K. H. Panofsky and M. Phillips, Classical Electricity and Magnetism, Reading, Massachusetts, Addison-Wesley Publishing Company, Inc., 1955.
22. R. E. Collin, Field Theory of Guided Waves, New York, McGraw-Hill Book Company, Inc., 1960
23. R. W. Grow, "Theoretical Propagation and Impedance Characteristics of a Finite Number of Coupled Ladders," 18th Annual Conference on Electron Tube Research, Washington University, Seattle, Washington, June 29, 30, and July 1, 1960.
24. L. S. Bowman and R. W. Grow, "Microwave Propagation in a Circuit Consisting of Four Coupled Ladders," Technical Report ONR-1, University of Utah, May 1, 1961.
25. R. L. Thurston, "Beam Coefficient for a Coupled-Ladder Traveling Wave Tube," B. S. Thesis, University of Utah, June 1962.

DISTRIBUTION LIST

| <u>NO. OF COPIES</u> | <u>AGENCY</u> | <u>NO. OF COPIES</u> | <u>AGENCY</u> |
|--------------------------|---|--------------------------|--|
| 2 | Asst. Sec. of Defense for Research and Development Information Office Library Branch Pentagon Building Washington 25, D. C. | 5 | Armed Services Technical Information Agency Documents Service Center Arlington Hall Station Arlington 12, Virginia |
| 6 | Director, Naval Research Laboratory Technical Information Officer (Code 2000) Washington 25, D. C. | 2 | Chief of Naval Research Electronics Branch (Code 427) Department of the Navy Washington 25, D. C. |
| 1 | Commanding Officer ONR Branch Office The John Crerar Library Building 86 E. Randolph Street Chicago 1, Illinois | 1 | Commanding Officer ONR Branch Office 346 Broadway New York 13, New York |
| 1 | Commanding Officer ONR Branch Office 1030 East Green Street Pasadena 1, California | 2 | Commanding Officer Office of Naval Research Navy #100, Fleet Post Office New York, New York (Box 39) |
| 1 | Electronics Research Directorate Library Air Force Cambridge Research Center Laurence G. Hanscom Field Bedford, Massachusetts | 1 | Office of Technical Services Technical Reports Sections Department of Commerce Washington 25, D. C. |
| 1 | Commander Air Force Office of Scientific Research Washington 25, D. C. ATTN: SRY | 1 | Office of Ordnance Research Box CM, Duke Station Durham, North Carolina |
| 1 | Technical Information Officer Signal Corps Engineering Laboratory Fort Monmouth, New Jersey | 1 | Director National Science Foundation Washington 25, D. C. |
| 1 | Director, Naval Research Laboratory (Code 6430) Washington 25, D. C. | 1 | Director, Naval Research Laboratory (Code 5220) Washington 25, D. C. |
| 2 | Chief, Bureau of Ships (Code 816c) Department of the Navy Washington 25, D. C. | 1 | Librarian U.S. Naval Ordnance Laboratory White Oak, Maryland |

| <u>NO. OF COPIES</u> | <u>AGENCY</u> | <u>NO. OF COPIES</u> | <u>AGENCY</u> |
|----------------------|--|----------------------|---|
| 1 | Chief, Bureau of Ships (Code 327) Department of the Navy Washington 25, D. C. | 1 | Director U. S. Naval Electronics Laboratory San Diego 52, California |
| 1 | Chief, Bureau of Aeronautics (Code EL-412.1) Department of the Navy Washington 25, D. C. | 1 | Chief, Bureau of Ordnance (Code RE P) Department of the Navy Washington 25, D. C. |
| 2 | Librarian, National Bureau of Standards Department of Commerce Washington 25, D. C. | 1 | Chief, Bureau of Ordnance (Code RE 9) |
| 1 | Advisory Group on Electron Tubes Secretary, Working Group on Semi- conductor Devices 346 Broadway New York 13, New York | 1 | Applied Physics Laboratory Johns Hopkins University Silver Spring, Maryland |
| 1 | Commanding Officer Wright Air Development Center Wright-Patterson Air Force Base, Ohio | 1 | Solid State Development Branch Evans Signal Laboratories Belmar, New Jersey |
| 1 | Research Laboratory for Electronics Massachusetts Institute of Technology Cambridge, Massachusetts | 1 | Solid State Group Hughes Aircraft Co. Research and Development Laboratories Culver City, California |
| 1 | Navy Representative, Project Lincoln Massachusetts Institute of Technology Building B, Lincoln Laboratory P. O. Box 73 Lexington 73, Massachusetts | | |
| 1 | Commanding Officer U. S. Army Signal Research and Development Laboratories Fort Monmouth, New Jersey ATTN: SIGRA/SL-PFA | | |
| 1 | Library U. S. Naval Ordnance Plant Indianapolis, Indiana | | |